

Study of heavy-flavor quarks produced in association with top-quark pairs at $\sqrt{s} = 7$ TeV using the ATLAS detector

(Dated: October 9, 2018)

Using a sample of dilepton top-quark pair ($t\bar{t}$) candidate events, a study is performed of the production of top-quark pairs together with heavy-flavor (HF) quarks, $t\bar{t} + b + X$ or $t\bar{t} + c + X$, collectively referred to as $t\bar{t} + \text{HF}$. The dataset used corresponds to an integrated luminosity of 4.7 fb^{-1} of proton–proton collisions at a center-of-mass energy of 7 TeV recorded by the ATLAS detector at the CERN Large Hadron Collider. The presence of additional HF quarks in the $t\bar{t}$ sample is inferred by looking for events with at least three b -tagged jets, where two are attributed to the b -quarks from the $t\bar{t}$ decays and the third to additional HF production. The dominant background to $t\bar{t} + \text{HF}$ in this sample is $t\bar{t} + \text{jet}$ events in which a light-flavor jet is misidentified as a heavy-flavor jet. To determine the heavy- and light-flavor content of the additional b -tagged jets, a fit to the vertex mass distribution of b -tagged jets in the sample is performed. The result of the fit shows that 79 ± 14 (stat.) ± 22 (syst.) of the 105 selected extra b -tagged jets originate from HF quarks, three standard deviations away from the hypothesis of zero $t\bar{t} + \text{HF}$ production. The result for extra HF production is quoted as a ratio (R_{HF}) of the cross section for $t\bar{t} + \text{HF}$ production to the cross section for $t\bar{t}$ production with at least one additional jet. Both cross sections are measured in a fiducial kinematic region within the ATLAS acceptance. R_{HF} is measured to be $[6.2 \pm 1.1(\text{stat.}) \pm 1.8(\text{syst.})]\%$ for jets with $p_{\text{T}} > 25$ GeV and $|\eta| < 2.5$, in agreement with the expectations from Monte Carlo generators.

PACS numbers: 14.65.Ha, 14.65.Fy, 14.65.Dw, 14.80.Bn, 13.85.Qk

I. INTRODUCTION

In order to characterize the recently observed Higgs-like particle (H) [1, 2], quantities such as the Yukawa coupling of the top quark and the Higgs boson need to be measured with precision. For a Standard Model (SM) Higgs boson with a mass of 125 GeV, the decay mode with the largest branching ratio is $H \rightarrow b\bar{b}$. Thus, the channel with the largest yields for studying $t\bar{t} + H$ production is $t\bar{t} + H, H \rightarrow b\bar{b}$. Production of top-quark pair ($t\bar{t}$) events featuring additional heavy-flavor (HF) b - and c -quarks, $t\bar{t} + b + X$ and $t\bar{t} + c + X$, referred to as $t\bar{t} + \text{HF}$, is the main irreducible background to $t\bar{t} + H, H \rightarrow b\bar{b}$. A study of $t\bar{t} + \text{HF}$ production is useful to constrain models of heavy-flavor quark production at the scale of the top-quark mass. This analysis is also of interest because of the many potential phenomena beyond the SM, such as composite Higgs models [3] and processes leading to final states with four top quarks [4–9], that could produce additional heavy-flavor quarks in the $t\bar{t}$ candidate sample.

This paper describes a study of $t\bar{t} + \text{HF}$ production. Within the SM, heavy-flavor quark pairs, $c\bar{c}$ and $b\bar{b}$, are expected to be produced in association with $t\bar{t}$ mainly via gluon splitting from initial- and final-state radiation [10]. In addition, the heavy-flavor content of the proton could lead to $t\bar{t}$ final states with at least one additional HF quark, $t\bar{t} + c$ and $t\bar{t} + b$. The data analyzed correspond to an integrated luminosity of 4.7 fb^{-1} at a center-of-mass energy of $\sqrt{s} = 7$ TeV produced at the Large Hadron Collider (LHC) and recorded in 2011 with the ATLAS detector.

This analysis is performed on $t\bar{t}$ dilepton candidate events in which each top quark decays to a b -quark and a W boson, which subsequently decays to a neutrino and an isolated, charged lepton. The dilepton signature

is selected for this measurement because it is relatively background free and precludes a third b -tagged jet from a hadronically decaying W boson, predominantly via $W \rightarrow s\bar{c}$. The $t\bar{t} + \text{HF}$ signal region is the subset of these events with three or more jets identified as containing HF quarks (b -tagged jets, or b -tags). However, jets without HF quarks may also be b -tagged, so that care must be taken to properly identify the flavor composition of the b -tagged jets in the sample. Two b -tagged jets from each event are presumed to originate from the b -quarks from top-quark decays, $t\bar{t} \rightarrow W^+bW^-\bar{b}$. Therefore, all events in the signal region have at least one additional b -tag either from a b - or c -quark jet, or from a light-quark or gluon jet that was misidentified. The latter are referred to as light-flavor or LF jets.

Due to limited data statistics and discrimination between b - and c -jets, the sum of b -quark and c -quark jet rates is measured. Information about the composition of $t\bar{t} + b + X$ and $t\bar{t} + c + X$ in $t\bar{t} + \text{HF}$ is nevertheless required for the total correction due to acceptance, which is different for b - and c -quark jets. The composition is estimated with Monte Carlo simulation and tested in the data.

From the measurement of the fraction of jets with heavy flavor content, the cross section for $t\bar{t}$ production with at least one additional HF jet can be extracted. To reduce some systematic uncertainties, the result is quoted as a ratio, termed R_{HF} , of the cross section for $t\bar{t}$ production with at least one additional HF jet to the cross section for $t\bar{t}$ production with at least one additional jet ($t\bar{t} + j$), regardless of flavor. The measurement of $t\bar{t} + j$ production is performed in dilepton $t\bar{t}$ candidate events with at least three jets, at least two of which are b -tagged and assumed to come from top-quark decays.

The paper is organized as follows. The ATLAS

detector is briefly described in Sec. II. The data and Monte Carlo samples used in the analysis are described in Sec. III, followed by a description of the event selection in Sec. IV. The definition of the fiducial phase space used in the measurement of R_{HF} , and the calculation of acceptances and efficiencies are presented in Sec. V. In Sec. VI, observed and expected numbers of events with ≥ 3 b -tagged jets are shown. Section VII describes a fit to the vertex mass distribution of b -tagged jets in these data events to extract the fraction of HF jets produced in association with $t\bar{t}$. A discussion of the systematic uncertainties of the measurement is presented in Sec. VIII. Section IX shows the result of the measurements, followed by conclusions in Sec. X.

II. THE ATLAS DETECTOR

A detailed description of the ATLAS detector can be found elsewhere [11]. The innermost part of the detector is a tracking system that is immersed in a 2 T axial magnetic field and that measures the momentum of charged particles. The inner detector comprises a silicon pixel detector, a silicon microstrip detector, and a transition radiation tracker, providing tracking capability within the pseudorapidity range $|\eta| < 2.5$ [12]. The tracking system is also used to identify the displaced secondary vertex that is formed by hadrons containing a b - or c -quark. Calorimeter systems, which measure the electron, photon, and hadron energies, reside outside the inner detector and cover the region $|\eta| < 4.9$. Outside the calorimeters there is a muon spectrometer that is used to identify and measure the momentum of muons in an azimuthal magnetic field in the region $|\eta| < 2.7$. To reduce the data rate, a three-level trigger system selects the potentially interesting events that are recorded for offline analysis.

III. DATA AND MONTE CARLO SAMPLES

The total integrated luminosity for the analyzed data sample is 4.7 fb^{-1} at a center-of-mass energy of $\sqrt{s} = 7 \text{ TeV}$. During the 2011 data-taking period the instantaneous luminosity of the LHC increased, causing the average number of simultaneous inelastic pp interactions per beam crossing (pile-up) at the beginning of a pp fill to increase from about 6 to 17. Multiple pp interactions can occur either in the same bunch crossing as the primary vertex (termed ‘in-time pile-up’) or in an adjacent bunch crossing (termed ‘out-of-time pile-up’). To account for these effects, all Monte Carlo simulated events are overlaid with additional inelastic events generated with the PYTHIA AMBT1 tune [13], and the distribution of the number of vertices in the simulation is reweighted to match the distribution of

the number of additional interactions per bunch crossing measured in the data.

Monte Carlo simulation is used to study signal and background processes. Inclusive $t\bar{t}$ production and dedicated $t\bar{t} + \text{HF}$ samples are simulated using the multi-leg matrix-element generator ALPGEN v2.13 [14] with the CTEQ6L1 [15] parton distribution function (PDF) set. Parton showering and hadronization are performed by HERWIG v6.520 [16]. Effects due to the mass of the heavy-flavor quarks are included by default in ALPGEN. In these samples, additional jets (including heavy-flavor) can also be produced in the parton shower. The MLM [14] parton-jet matching scheme is applied to avoid double counting of configurations generated by both the parton shower and the leading-order (LO) matrix-element (ME) calculation. In addition, overlap between $t\bar{t}$ events with HF quarks that originate from ME production and those that originate from the parton shower is removed. This heavy flavor overlap removal (HFOR) is based on the ΔR_{qq} [17] between simulated HF quarks. The event is taken from the ME calculation if it contains two well separated HF quarks ($\Delta R_{qq} > 0.4$). The event is taken from the parton shower calculation if it contains two collinear HF quarks ($\Delta R_{qq} < 0.4$).

To study the effect of different fixed-order calculations and matching schemes, samples of top-quark pair events are also generated using POWHEG v1.01 and showered with HERWIG. In this sample the $t\bar{t}$ process is described at next-to-leading order (NLO), while the extra jets are described at LO. For each sample showered with HERWIG, JIMMY v4.31 [18] and the AUET1 tune [19] are used to simulate the underlying event and to model various soft interactions. To assess the effect of different parton shower models, a sample is generated using ALPGEN v2.14 with the PYTHIA v6.425 [20] parton shower and hadronization, using the CTEQ5L PDF set [21]. The uncertainty associated with the CTEQ6L1 PDF set is evaluated with an envelope calculated using the uncertainty set from the NLO PDF MTSW2008nlo68cl [22], and an additional term to account for the difference between the central values of the LO and NLO calculations.

Initial- and final-state radiation (ISR/FSR) variations are studied using samples generated with ACERMC v2.0 [23] interfaced with PYTHIA v6.2. In these samples the parameters that control the amount of ISR/FSR are set to points consistent with the PERUGIA Hard/Soft tune [24] in a range constrained by current experimental data [25].

In all samples the top-quark mass is set to $m_t = 172.5 \text{ GeV}$. The cross section for Standard Model $t\bar{t}$ production at this mass is calculated using the approximate next-to-next-to-leading-order (NNLO) QCD calculation described in [26].

Background samples from the production of W and Z bosons are generated using the CTEQ6L1 PDFs with

ALPGEN, which is interfaced to HERWIG for parton showering and hadronization; the ALPGEN matrix elements include diagrams with up to five additional partons. Separate samples of $W + b\bar{b}$ and $Z + b\bar{b}$ events are generated. The overlap between jets from the parton-shower and the matrix-element in the n and $n + 1$ jet multiplicity samples is removed for the W +jets and Z +jets samples in the same manner as for the $t\bar{t}$ samples. Single top-quark production is modeled using ACERMC in the t -channel and MC@NLO v3.41 [27] for the Wt - and s -channels. Diboson (WW , WZ , and ZZ) production is modeled using ALPGEN interfaced with HERWIG. Less than 0.5% of the expected yield in the $t\bar{t} + \text{HF}$ sample comes from the associated production of $t\bar{t} + W/Z$ and $t\bar{t} + H$, and these processes are thus neglected in this analysis.

The resulting generated samples are passed through a GEANT4 simulation [28] of the ATLAS detector [29]. Events are then reconstructed in the same manner as the data.

IV. EVENT SELECTION

Events for the analysis are selected by at least one of the high- p_T [12] single-electron or single-muon triggers, as described in Refs. [30] and [31]. The single-electron triggers are based on calorimeter energy deposits, shower shape, and matching track quality constraints, while the single-muon triggers are based on a reconstructed track in the muon spectrometer that matches a track found in the inner detector. To ensure a final trigger rate that is compatible with the ATLAS data acquisition system, a minimum p_T threshold for the electron and muon triggers is used. The p_T threshold for the muon trigger is 18 GeV. For the electron trigger, the threshold is 20 GeV or 22 GeV, depending on the data-taking period due to varying LHC luminosity conditions.

The selected events are required to contain a reconstructed primary vertex with at least five associated tracks with $p_T > 0.4$ GeV. Event reconstruction makes use of electrons (e), muons (μ), jets, and missing transverse momentum (E_T^{miss}). Electrons are reconstructed by matching energy deposits in the electromagnetic calorimeter with tracks in the inner detector, and are required to have $p_T > 25$ GeV and $|\eta| < 2.47$, excluding the transition region between the barrel and end-cap calorimeters at $1.37 < |\eta| < 1.52$ [32]. Muons are reconstructed by matching tracks in the inner detector with tracks measured in the muon spectrometer, and are required to have $p_T > 20$ GeV and $|\eta| < 2.5$.

Tight isolation cuts are applied to both the electron and muon candidates to reduce the number of identified leptons (e , μ) that come from non-prompt (non- W/Z) sources and from misidentified hadrons. For electrons, the E_T deposited in the calorimeter cells in a cone in η -

ϕ space of radius $\Delta R = 0.2$ around the electron position is summed, and the E_T due to the electron is subtracted. The scalar sum of track transverse momenta in a cone of $\Delta R = 0.3$, excluding the electron, is also measured. Cuts parametrized by the electron η and E_T are made on these two isolation variables to ensure a constant efficiency over the entire (η, E_T) range. For muons, the corresponding calorimeter isolation energy in a cone of $\Delta R = 0.2$ is required to be less than 4 GeV, and the scalar sum of track transverse momenta in a cone of $\Delta R = 0.3$ is required to be less than 2.5 GeV after subtraction of the muon p_T .

Jets are reconstructed from clustered energy deposits in the calorimeters with the anti- k_r [33] algorithm with a radius parameter $R = 0.4$ [34]. Jets selected for the analysis are required to have $p_T > 25$ GeV and $|\eta| < 2.5$. In order to reduce the background from jets originating from pile-up interactions, additional selection criteria are applied to the fraction of the jet's p_T (JVF) carried by tracks originating from the primary vertex, $JVF > 0.75$.

The transverse momentum of neutrinos produced in the top-quark decays, measured as E_T^{miss} , is inferred by balancing the vector sum of all visible transverse momenta. Specifically, the E_T^{miss} is constructed from the vector sum of all calorimeter cell energies contained in topological clusters [34] with $|\eta| < 4.5$, projected onto the transverse plane. Contributions to the E_T^{miss} from the calorimeter cells associated with jets are taken at the corrected energy scale that is used for jets, while the contribution from cells associated with electrons is substituted by the calibrated transverse momentum of the electron. The contribution to the E_T^{miss} from the p_T of muons passing the selection requirements is also included.

The b -tagging algorithm [35, 36] employed for this analysis uses impact parameter and vertex position measurements from tracks in the inner detector as inputs to a neural network. The b -tagging efficiency was calibrated in a multi-jet data sample where at least one jet contains a muon [36]. The c -tagging efficiency was calibrated in a data sample with reconstructed D^* mesons [37]. For this analysis, b -tagged jets are required to satisfy a selection that is 75% efficient for b -quark jets, approximately 30% efficient for c -quark jets, and rejects light-flavor jets by a factor of approximately 35 in simulated $t\bar{t}$ events. In this paper, a ‘ b -tag’ (or a ‘ b -tagged jet’) refers to any jet passing this selection, regardless of flavor. A ‘ b -jet’, by contrast, refers to a jet (which may or may not be b -tagged) which contains a b -quark. Similarly, ‘ c -jet’ and ‘HF jet’ are statements of the flavor composition of the jet, not whether the jet is b -tagged. Three distinct subsets of the selected b -tagged jets with different b -jet purity are used in the measurement of $\sigma_{\text{fid}}(t\bar{t} + \text{HF})$, as described in Sec. VII.

Dilepton $t\bar{t}$ candidate events are selected by requir-

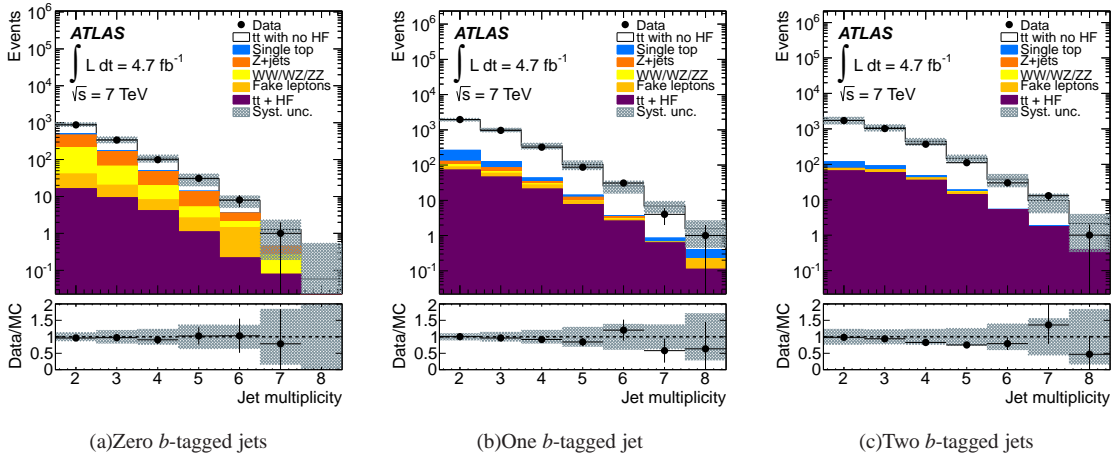


FIG. 1: Jet multiplicity distributions in dilepton $t\bar{t}$ candidate events with (a) zero, (b) one, or (c) two b -tagged jets for the sum of ee , $\mu\mu$ and $e\mu$ channels. The lower plots show the ratio between the data and the Monte Carlo predictions in each bin. Uncertainties are statistical and systematic. The last bin contains any overflow.

ing exactly two opposite-sign leptons and at least two jets. To reduce the background from Z/γ^* processes, events with like-flavor leptons are required to have E_T^{miss} above 60 GeV and a dilepton invariant mass satisfying $|m_{\ell^+\ell^-} - m_Z| > 10$ GeV. For events with one electron and one muon, the scalar sum of the lepton and jet transverse momenta is required to be above 130 GeV to reduce the backgrounds from $Z/\gamma^* \rightarrow \tau^+\tau^-$, as well as WW , WZ , and ZZ processes. This set of selection criteria is termed the ‘nominal’ $t\bar{t}$ selection criteria. The measurement of $t\bar{t} + \text{HF}$ production is carried out in the subset of these events that contain three or more b -tagged jets, whereas the measurement of $t\bar{t}$ production with at least one additional jet is performed in the subset with at least three jets, at least two of which are b -tagged.

Using the nominal selection criteria described above, data and Monte Carlo events are compared in three control regions: dilepton $t\bar{t}$ candidate events with zero, one, or two b -tagged jets. Data-to-simulation normalization corrections are applied to Monte Carlo simulation samples when calculating acceptances to account for observed differences in predicted and observed trigger and lepton reconstruction efficiencies, jet flavor tagging efficiencies and mistag rates, as well as jet and lepton energy scales and resolutions. In Fig. 1, the jet multiplicity distributions in the three regions are compared to Monte Carlo predictions. Agreement is observed within uncertainties.

V. DEFINITION OF THE FIDUCIAL PHASE SPACE AND CALCULATION OF CORRECTION FACTORS

To allow comparison of the analysis results to theoretical predictions, the measurement is made within

a fiducial phase space. The fiducial volume is defined in Monte Carlo simulation by requiring two leptons (e , μ) from the $t \rightarrow Wb \rightarrow \ell\nu b$ decays (including electrons and muons coming from $\tau \rightarrow \ell\nu\nu_\tau$) with $p_T > 25$ (20) GeV for e (μ), and $|\eta| < 2.5$ as well as three or more jets with $p_T > 25$ GeV and $|\eta| < 2.5$.

In the simulation, jets are formed by considering all particles with a lifetime longer than 10 ps, excluding muons and neutrinos. Particles arising from pile-up interactions are not considered. For the determination of the $t\bar{t} + \text{HF}$ fiducial cross section, $\sigma_{\text{fid}}(t\bar{t} + \text{HF})$, three or more jets are required to match a b - or c -quark, two of which must match a b -quark from top-quark decay. All simulated b - and c -quarks that were generated with $p_T > 5$ GeV are considered for the matching, and are required to satisfy $\Delta R(\text{quark}, \text{jet}) < 0.25$. Jets that match both a b - and a c -quark are considered as b -jets. For the calculation of $\sigma_{\text{fid}}(t\bar{t} + j)$ three or more jets are required, two of which must contain a b -quark from top-quark decay.

Each fiducial cross section is determined using measured quantities from the data, and a correction factor derived from the Monte Carlo simulation. The ratio of cross sections is defined as:

$$R_{\text{HF}} = \frac{\sigma_{\text{fid}}(t\bar{t} + \text{HF})}{\sigma_{\text{fid}}(t\bar{t} + j)}$$

The fiducial cross section for $t\bar{t} + \text{HF}$ production is determined from:

$$\sigma_{\text{fid}}(t\bar{t} + \text{HF}) = \frac{N_{\text{HF}}}{\int \mathcal{L} dt \cdot \epsilon_{\text{HF}}}; \quad (1)$$

where N_{HF} is the number, after background subtraction, of b -tags from HF jets observed in the data, in addition

to the two b -jets from top-quark decays. The integrated luminosity of the sample is denoted as $\int \mathcal{L} dt$, and ϵ_{HF} is a correction factor taken from Monte Carlo simulation that converts the number of observed b -tags from additional HF jets to the number of events in the signal fiducial volume. This correction factor includes the acceptance within the fiducial region, the reconstruction efficiency, and a factor to account for the multiplicity of extra b -tagged HF jets per $t\bar{t}$ +HF event in the signal region. This correction factor is different for $t\bar{t} + b + X$ (ϵ_b) and $t\bar{t} + c + X$ (ϵ_c), and thus ϵ_{HF} is determined as a weighted sum of these two contributions. The weight used to form the sum is the fraction of $t\bar{t} + \text{HF}$ events in the fiducial volume which contain additional b -jets as opposed to c -jets. This fraction is termed $F_{b/\text{HF}}$. The total correction factor (ϵ_{HF}) is calculated as:

$$\epsilon_{\text{HF}} = F_{b/\text{HF}} \cdot \epsilon_b + (1 - F_{b/\text{HF}}) \cdot \epsilon_c$$

The denominator for R_{HF} , $\sigma_{\text{fid}}(t\bar{t} + j)$, is computed using a similar prescription:

$$\sigma_{\text{fid}}(t\bar{t} + j) = \frac{N_j}{\int \mathcal{L} dt \cdot \epsilon_j}; \quad (2)$$

where N_j is the yield of dilepton events in data with at least three jets, at least two of which are b -tagged, and ϵ_j is the $t\bar{t} + j$ acceptance factor calculated from the Monte Carlo simulation. The acceptance calculation for each fiducial cross section assumes that all b -tagged jets are from real HF quarks. Events with b -tagged jets from LF quarks are treated as a background, and subtracted when computing both N_{HF} and N_j .

The ALPGEN + HERWIG Monte Carlo sample predicts $\epsilon_b = 0.19$, $\epsilon_c = 0.06$, and $F_{b/\text{HF}} = 0.31$. The total correction factor is thus predicted to be $\epsilon_{\text{HF}} = 0.106 \pm 0.005$ (stat.) for $\sigma_{\text{fid}}(t\bar{t} + \text{HF})$. For $\sigma_{\text{fid}}(t\bar{t} + j)$ the acceptance factor is calculated to be $\epsilon_j = 0.129 \pm 0.001$ (stat.).

The prediction for R_{HF} from the ALPGEN + HERWIG Monte Carlo sample is 3.4%. The value obtained from the POWHEG v1.01 [38] generator showered with HERWIG [16] is $R_{\text{HF}} = 5.2\%$, with $F_{b/\text{HF}} = 0.34$. While this R_{HF} value is different to that from ALPGEN + HERWIG, the predicted $F_{b/\text{HF}}$ values are similar. Furthermore, a parton-level study using MADGRAPH5 v1.47 [39] gives $F_{b/\text{HF}} = 0.29$. The value of $F_{b/\text{HF}}$ is also stable when different showering algorithms are used: the ALPGEN + PYTHIA Monte Carlo sample predicts a value of $F_{b/\text{HF}} = 0.32$, in good agreement with the prediction when HERWIG is used. Based on comparison of these predictions for $F_{b/\text{HF}}$, a symmetric 10% Monte Carlo systematic uncertainty is assigned, $F_{b/\text{HF}} = 0.31 \pm 0.03$. The prediction of $F_{b/\text{HF}}$ is also tested in data (see Sec. IX).

VI. EXPECTED SIGNAL AND BACKGROUND YIELDS

Table I shows the number of events with ≥ 3 b -tagged jets expected in the Monte Carlo simulation from dilepton $t\bar{t}$ production and from various background sources. At this point, no distinction is made between events with a true additional HF jet and those containing a mistagged LF jet. The number of observed events is also shown. While Monte Carlo simulation is used to estimate $t\bar{t} + \text{HF}$ event rates and kinematic features, data-driven methods and Monte Carlo simulation are both used to estimate background processes, as detailed below.

Background processes containing real b -jets and leptons, such as single top-quark, $Z/\gamma^* + \text{jets}$, and diboson (WW , WZ , and ZZ) production, are estimated using Monte Carlo simulation. Contributions from diboson production are found to be negligible.

A major source of background comes from $t\bar{t}$ events in which one or more of the b -tagged jets is from a mistagged LF jet. This background is estimated using Monte Carlo simulation for the measurement of $\sigma_{\text{fid}}(t\bar{t} + j)$. However, in the measurement of $\sigma_{\text{fid}}(t\bar{t} + \text{HF})$, the final $t\bar{t} + \text{LF}$ background is determined by a fit to the vertex mass distribution of b -tagged jets in data, as explained in Sec. VII.

Background from events in which at least one of the leptons is either non-prompt (originating from e.g. a photon conversion or b -quark decay) or is a misidentified hadron, is estimated using data and Monte Carlo simulation. For instance, $W + \text{jets}$, multi-jet, and $t\bar{t}$ events with one hadronically decaying W boson can contribute in this way. This contribution is determined by scaling the yield of events in the data with a pair of same-sign leptons by the ratio of opposite-sign to same-sign yields ($R_{\text{OS/SS}}$) obtained in Monte Carlo simulation. The opposite-sign to same-sign ratio is determined separately for the three dilepton channels, and found to be 1.3 ± 0.1 (stat.) $^{+1.8}_{-1.3}$ (syst.) for e^+e^- events, 1.2 ± 0.1 (stat.) ± 0.7 (syst.) for $\mu^+\mu^-$ events, and 1.2 ± 0.1 (stat.) ± 0.5 (syst.) for events with one electron and one muon. The systematic uncertainty takes into account the unknown relative mixture of fake-lepton sources (photon conversions, b - and c -hadron decays, or misidentified hadrons) in the $R_{\text{OS/SS}}$ calculation. Since the central value of the prediction for this background is zero events, only variations in $R_{\text{OS/SS}}$ that lead to larger background predictions are considered in the systematic uncertainty calculation. This method for estimating the background due to events with fake leptons is validated in a control sample of dilepton events with less restrictive lepton identification requirements and no isolation criteria.

The dominant uncertainties on the total yield in Table I come from the jet energy scale, b -tagging efficiency, parton showering model, and initial- and final-

TABLE I: Observed and expected number of events in the signal region (i.e. with ≥ 3 b -tagged jets). Uncertainties on individual components are statistical only. For the total expectation, systematic uncertainties are included.

Process	Number of events
$t\bar{t}$	106.7 ± 3.4
Single top	2.2 ± 0.5
Z + jets	0.2 ± 0.1
Fake leptons	0^{+5}_{-0}
Total expectation	109^{+6}_{-3} (stat.) ± 35 (syst.)
Data	106

state radiation.

VII. TEMPLATE FIT

For the measurement of $\sigma_{\text{fid}}(t\bar{t} + \text{HF})$, the fraction of heavy-flavor jets produced in association with $t\bar{t}$ is extracted by performing a binned maximum-likelihood fit on the displaced-vertex mass distribution using all b -tagged jets in the events with ≥ 3 b -tagged jets. Although the final result is for both flavors combined, the fit includes separate b - and c -quark components to improve the determination of the LF fraction, and to test the Monte Carlo prediction for $F_{b/\text{HF}}$, which is used for the calculation of the correction factor described in Sec. V. This displaced-vertex mass is constructed from the inner detector tracks associated with the secondary vertex using the algorithm described in Ref. [40]. While the presence of a displaced vertex is an indication that a jet contains a b -quark, a jet may be b -tagged even if no vertex is reconstructed. In this case, the vertex mass is undefined. These jets are assigned a mass value of ‘ -1 GeV’ and they are included in the fit to the displaced-vertex mass distribution. Keeping the events without a reconstructed vertex improves the discrimination between heavy-flavor and light-flavor jets.

While the vertex mass is a powerful discriminant, Monte Carlo studies indicate that the sensitivity on the fitted fraction of LF jets increases when the jet p_{T} is used as an additional discriminant. Considering only the statistical uncertainty, it is seen that a fit with both jet p_{T} and vertex mass is approximately half a standard deviation more sensitive than a fit with only the vertex mass. It was thus decided to define a two-dimensional probability density function, termed a ‘template,’ for the fit using the vertex mass and jet p_{T} .

The fit is performed simultaneously in three *mutually exclusive* bins of b -jet purity, defined by different ranges of the b -tagging neural network output value. Certain values of the neural network output, termed ‘operating points’, are defined by the average b -jet selection efficiency resulting from the applied selection.

TABLE II: Summary of the b -tagging efficiencies for b -jets, c -jets, and light-flavor jets for the three *mutually exclusive* b -tagging selections used in the vertex mass template fit.

b -purity	b -jet efficiency	c -jet efficiency	light-flavor efficiency
High	60%	17%	0.43%
Medium	10%	7%	1.00%
Low	5%	6%	1.33%

In this analysis, operating points of 60%, 70% and 75% efficiency are used to define the boundaries of the b -jet purity bins.

The first bin uses only the tightest calibrated operating point (60%), contains the highest-purity sample of b -jets (referred to as ‘high purity’), and has a b -tagging efficiency of 60% for b -jets. The second bin (referred to as ‘medium purity’) requires a b -tag selection between the tightest and second tightest (70%) operating points, and contains a larger fraction of LF jets and c -jets. The efficiency for this bin is 10% for b -jets, i.e. the difference between the 70% and 60% operating points. The final bin (‘low purity’) requires a b -tag selection between the second (70%) and third operating point (75%), and contains the largest fraction of LF jets. The efficiency for this bin is 5% for b -jets. The b -tagging efficiencies for b -jets, c -jets, and light-flavor jets for each selection are given in Table II.

All three classes of b -tag purity are used in the analysis so that a jet is considered ‘ b -tagged’ if it satisfies any of these criteria. The discrimination power between LF and c -jets is greatly improved by using three (as opposed to one) classes of b -purity. The vertex mass distributions for all b -tagged jets in events passing the nominal $t\bar{t}$ selection criteria are shown in Fig. 2 to confirm that (a) the data are well described by the Monte Carlo simulation, (b) and the b -jet, c -jet and LF-jet fractions are different in the three purity selections. For the purpose of illustration, the normalization of the b -jet, c -jet, and LF-jet components is taken from Monte Carlo simulation.

The template fit has five components: b -jets from top-quark decays, non- $t\bar{t}$ background, extra b -tagged jets from b -quarks, extra b -tagged jets from c -quarks, and light-flavor b -tagged jets. The template for b -jets from top-quark decays is obtained from the data in $t\bar{t}$ dilepton events with exactly two b -tags. Monte Carlo simulation indicates that 97% of b -tagged jets in $t\bar{t}$ dilepton events with exactly two b -tags come from the decay of the top quark. To account for this in the shape of the data template, a template for b -tags not from the top-quark decays is derived from the $t\bar{t}$ Monte Carlo simulation, and subtracted with a 3% relative normalization from the data template. In the fit, the normalization for the template for b -jets from the top-quark decays is fixed assuming it contributes two of the three or more b -tags per observed event.

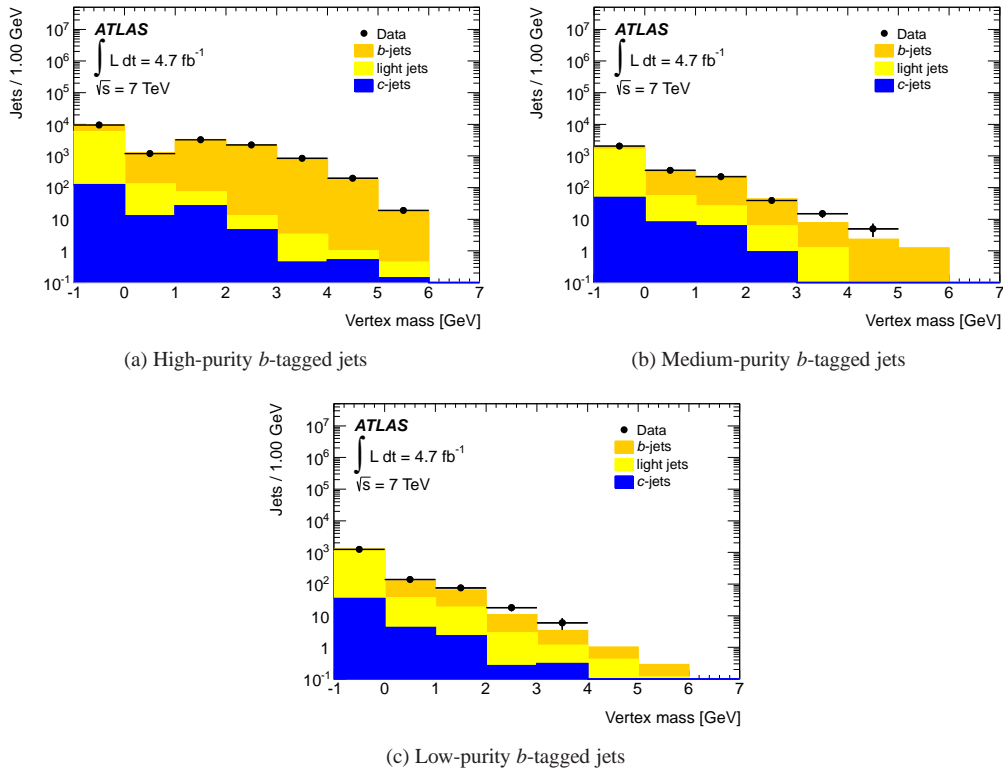


FIG. 2: Vertex mass distributions for all b -tagged jets in data events satisfying the nominal dilepton $t\bar{t}$ event selection, with no requirement on b -tagged jet multiplicity, compared to Monte Carlo predictions. By definition, jets with no reconstructed secondary decay vertex are assigned to the ‘ -1 GeV’ bin.

Background events from non-dilepton $t\bar{t}$ processes are included using Monte Carlo simulation, and enter the fit with a fixed normalization. Monte Carlo simulation is used to obtain templates for additional (non- $t \rightarrow Wb$) b -jets, c -jets, and LF jets.

In the fit to determine the number of b -tags from HF jets in addition to the two b -jets from top-quark decay, N_{HF} , separate templates for each category of jet in each of the three purity classes (high, medium, and low) are used. The b -tagging efficiencies (Table II) for each flavor of jet are used to relate the number of jets in each purity bin. After the application of all constraints, the fit has two floating parameters: the fraction of LF jets and the fraction of additional b -jets. The fraction of additional c -jets makes up the remainder.

Monte Carlo pseudo-experiments show that the fitting method is unbiased in both best-fit values and estimated uncertainties. The fit strategy (including estimates of statistical and systematic uncertainties) was verified using 10% of the full data sample as well as with Monte Carlo pseudo-experiments before the fit was performed on the full data sample. These studies indicated that the fit could achieve only a 1σ separation of b - vs. c - jets based on the expected statistical uncertainty alone. Inclusion of the systematic uncertainty would further reduce the sensitivity. However, the LF-

jet fraction is expected to be measured with sufficient precision to give a statistically significant measurement of the total HF content, defined as the fraction of additional b -tagged jets not coming from LF jets. In the fit, the individual fractions are not constrained to be positive or below unity.

VIII. SYSTEMATIC UNCERTAINTIES

Systematic uncertainties may affect the shape of the vertex mass and p_T templates as well as the acceptance calculations. For the systematic uncertainties on the template shapes, the fit to the data is re-evaluated using new templates, derived by varying the relevant parameters by their systematic uncertainties, and a new fit to the data is performed. Major uncertainties that affect the fit are the jet energy scale and resolution, the tagging efficiencies for b -, c - and LF jets, the parton-shower and hadronization models, and the Monte Carlo event generators.

The template for b -jets from top-quark decays is nominally taken from the data with exactly two b -tags. To account for kinematic biases due to additional heavy-flavor jets in the event, a systematic uncertainty on the shape of this template is assessed using b -jets

from top-quark decays from Monte Carlo inclusive $t\bar{t}$ events with three or more b -tagged jets.

The vertex mass of additional b - and c -jets is sensitive to the number of HF quarks contained in a jet (for instance, for $b\bar{b}$ or $c\bar{c}$ produced via gluon splitting). The dominant uncertainty from this effect would manifest itself as a difference in the shape of the template for additional b -jets. To assess this uncertainty, the template for additional b -jets is replaced by the template for b -jets from top-quark decays.

By default, the normalization of the template for b -jets from top-quark decays is fixed to two per event. A systematic uncertainty on this normalization is assessed by using the predicted normalization from Monte Carlo simulation, which includes events with less than two b -tags from top-quark decays, due to b -tagging inefficiency. The total uncertainty due to specific template shape variations is referred to as ‘additional fit uncertainties’ for the rest of this paper.

Systematic uncertainties also affect the overall event reconstruction efficiency. Dominant sources of uncertainty for this category are: the tagging efficiencies for b -, c - and LF jets, the jet energy scale and resolution, and the Monte Carlo event generator. Uncertainties on the lepton identification efficiency, E_T^{miss} reconstruction, and fragmentation modeling are negligible. In general, systematic uncertainties are evaluated on the full data sample, with each uncertainty being taken as the difference between the nominal and the varied resulting values of R_{HF} .

An important uncertainty in this analysis comes from the flavor composition in the fiducial volume, namely in the value of $F_{b/\text{HF}}$, the fraction of $t\bar{t}$ + HF events in the fiducial volume which contain b -jets, used to calculate the correction factor ϵ_{HF} . As described in Sec. V, an uncertainty of 10% on $F_{b/\text{HF}}$ is estimated using different Monte Carlo generators. It is possible to evaluate $F_{b/\text{HF}}$ using the data, but with the present data set, significant discrimination between b - and c -jets is not possible, making such a comparison of limited use. Nonetheless, the result of this study is presented as a point of comparison to the result obtained from the Monte Carlo.

IX. RESULTS

In the 106 events in the signal sample (with ≥ 3 b -tagged jets), there are 325 b -tagged jets. After subtracting the non- $t\bar{t}$ background component, and the contribution from the tagged jets from the $t \rightarrow Wb$ decay, the number of additional b -tags is found to be 105. As described in Sec. VII, a template fit to all b -tagged jets is performed to determine the flavor composition of these additional b -tagged jets. The result of the fit to all 325 b -tagged jets is shown in Fig. 3. The weighted sums of all fit templates are shown, with contributions for extra

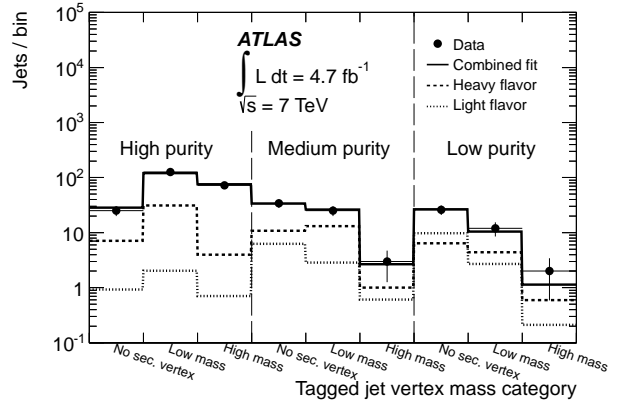


FIG. 3: The result of the template fit (solid line) to the vertex mass distribution in data (points). Data are divided into three groups depending on the purity of b -jets passing each selection, as described in the text. The first three bins are the vertex mass distributions for the high-purity b -tags, the middle three bins for the medium-purity b -tags, and the last three bins for the low-purity b -tags. Within each purity category, the first bin contains jets with no reconstructed secondary vertex. The middle bin contains jets with ‘low’ mass: less than 2 GeV. The third bin contains jets with ‘high’ mass: greater than 2 GeV. The best fit is shown as a sum (labeled as ‘Combined fit’, which includes the b -jets from top-quark decay) with separate contributions from additional b - and c -jets (labeled as ‘Heavy flavor’), and LF jets (labeled as ‘Light flavor’).

TABLE III: Relative composition of b -tagged jets in the signal region, fitted in data and compared to the expectation from Monte Carlo (MC) simulation. In data, the fractions of LF and additional b -jets are determined by the fit. The fraction of b -jets from top-quark decays is fixed in the fit to two b -tags in each event. The contributions from $t\bar{t}$ events with a fake lepton, or non- $t\bar{t}$ events are fixed in the fit using the Monte Carlo simulation (those are labeled as ‘ b -jets from other sources’ in the table). The fraction of c -jets is inferred from unitarity. All quoted errors are statistical.

Type of b -tag, fractions	Data fit	MC expectation
Additional LF jets, %	8 ± 4	20
Additional b -jets, %	-2 ± 7	9
Additional c -jets, %	26 ± 8	3.5
b -jets from $t \rightarrow Wb$, %	65	–
b -jets from other sources, %	2.5	–

HF and mistagged LF jets shown separately. The fitted fractions of b -tags from LF jets and additional b -jets are given in Table III. Of the 105 additional b -tags, 79 ± 14 (stat.) ± 22 (syst.) are attributed to HF jets. A detailed breakdown of the systematic uncertainties on the total number of HF jets is shown in Table IV.

Using Eq. 1, the number of HF jets observed in data, and the quoted correction factor ϵ_{HF} derived from

TABLE IV: Summary of systematic uncertainties (in %) on the measurement of the ratio of fiducial cross sections, R_{HF} . Uncertainties are quoted separately for the number of HF jets measured in the fit (N_{HF}), the portion of the calculation affecting only the correction factors (ϵ_{HF}), and the full calculation. As the fit prefers 100% charm for additional heavy-flavor jets, it is sensitive to differences in the extra b -tagged jets from the c -quark template shape.

Source	% (N_{HF})	% (ϵ_{HF})	% (full)
Lepton reconstruction	0.1	0.2	0.2
Jet reconstruction and calibration	3.5	1.6	6.9
$E_{\text{T}}^{\text{miss}}$ reconstruction	0.5	0.6	0.9
Fake-lepton estimate	3.4	0.0	3.4
Tagging efficiency for b -jets	1.1	2.4	3.1
Tagging efficiency for c -jets	25.0	5.9	21.2
Tagging efficiency for light jets	8.4	0.2	8.4
Fragmentation modeling	6.5	15.7	10.2
Generator variation	0.7	1.0	1.8
Initial- and final-state radiation	0.1	1.7	1.9
PDF uncertainties	1.6	1.0	2.8
Additional fit uncertainties	6.6	–	6.6
Fiducial flavor composition	0.0	6.0	6.0
Total systematic	29	13	28

the Monte Carlo simulation for $t\bar{t} + \text{HF}$ production, $\sigma_{\text{fid}}(t\bar{t} + \text{HF})$ is found to be 0.16 ± 0.03 (stat.) pb. ALPGEN interfaced with HERWIG predicts a value of 0.10 pb.

The uncertainty on the fitted fraction of light-flavor jets is significantly smaller than the uncertainty on the fitted fraction of additional b -jets. This is understood as an effect of fitting in multiple b -purity bins: the low-purity bin is dominated by light-flavor jets and thus gives improved discrimination. The data resolve the total observed HF production rate with a significance of about 3σ .

In the data, 1656 $t\bar{t}$ dilepton candidate events are observed with at least three jets, at least two of which are b -tagged. The total background estimate, which is dominated by LF jets misidentified as b -jets from top-quark decay, is found to be 112 ± 4 (stat.), leading to a background subtracted yield of 1544 ± 41 (stat.). Using Eq. 2, and the quoted acceptance factor for $t\bar{t} + j$ production, $\sigma_{\text{fid}}(t\bar{t} + j)$ is found to be 2.55 ± 0.07 (stat.) pb, compared to 2.83 pb predicted by ALPGEN and HERWIG. Taking into account the total uncertainty, it is found that $R_{\text{HF}} = [6.2 \pm 1.1$ (stat.) ± 1.8 (syst.)]%. A full breakdown of the systematic uncertainties contributing to R_{HF} is given in Table IV.

The extracted value of $\sigma_{\text{fid}}(t\bar{t} + \text{HF})$ is very sensitive to the value of $F_{b/\text{HF}}$. As indicated in Sec. V, the efficiency for $t\bar{t} + b + X$ events is approximately a factor of three higher than the corresponding efficiency for $t\bar{t} + c + X$ events, implying a potential change in $\sigma_{\text{fid}}(t\bar{t} + \text{HF})$ by a factor of three if $F_{b/\text{HF}}$ is allowed to vary

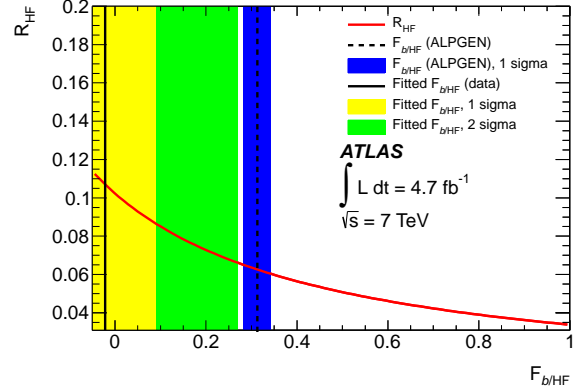


FIG. 4: The ratio R_{HF} of fiducial cross sections as a function of $F_{b/\text{HF}}$, the ratio of $t\bar{t}$ events with additional b -quarks to $t\bar{t}$ events with additional b - or c -quarks. The value of $F_{b/\text{HF}} = 0.31 \pm 0.03$ is indicated with a vertical dashed line with the band around it showing the 1σ uncertainty. The fitted fraction of additional b -jets is used to extract $F_{b/\text{HF}}$ (solid vertical line) from the data. The statistical uncertainty from the fit is used to define 1σ and 2σ uncertainty bands.

over the full range $[0, 1]$.

Using the fitted fraction of additional b -jets in data results in $F_{b/\text{HF}} = -0.02$, with one and two sigma statistical upper bounds of $F_{b/\text{HF}} = 0.09$ and 0.27 , respectively. This value is found to be compatible with the predicted value to within 1σ when systematic uncertainties are included. Figure 4 shows R_{HF} as a function of $F_{b/\text{HF}}$. The predicted and data-driven ranges of $F_{b/\text{HF}}$ are overlaid. With $F_{b/\text{HF}} = -0.02$ the central value for R_{HF} is determined as 10.7%.

X. CONCLUSIONS

A 4.7 fb^{-1} sample of 7 TeV proton–proton collisions recorded by the ATLAS detector at the LHC was used to measure the ratio R_{HF} of the fiducial cross section for the production of $t\bar{t}$ events with at least one additional HF quark jet ($t\bar{t} + b + X$ or $t\bar{t} + c + X$) to that for the production of $t\bar{t}$ events with at least one additional jet, regardless of flavor, each with $p_{\text{T}} > 25$ GeV and $|\eta| < 2.5$. A fit to the vertex mass distribution for b -tagged jets in $t\bar{t}$ candidate events with three or more b -tagged jets is performed to determine the heavy- and light-flavor content of the additional b -tagged jets. The result of the fit shows that 79 ± 14 (stat.) ± 22 (syst.) of the 105 selected b -tagged jets originate from HF quarks, three standard deviations away from the hypothesis of zero $t\bar{t} + \text{HF}$ production. A value of $R_{\text{HF}} = [6.2 \pm 1.1$ (stat.) ± 1.8 (syst.)]% is extracted. This value of R_{HF} is consistent with the leading order predictions of 3.4% obtained from the ALPGEN Monte Carlo generator interfaced with HERWIG and 5.2% from a calcu-

lation using POWHEG interfaced with HERWIG.

Acknowledgments

We thank CERN for the very successful operation of the LHC, as well as the support staff from our institutions without whom ATLAS could not be operated efficiently.

We acknowledge the support of ANPCyT, Argentina; YerPhI, Armenia; ARC, Australia; BMWF, Austria; ANAS, Azerbaijan; SSTC, Belarus; CNPq and FAPESP, Brazil; NSERC, NRC and CFI, Canada; CERN; CONICYT, Chile; CAS, MOST and NSFC, China; COLCIENCIAS, Colombia; MSMT CR, MPO CR and VSC CR, Czech Republic; DNRF, DNSRC and Lundbeck Foundation, Denmark; EPLANET and ERC, European Union; IN2P3-CNRS, CEA-DSM/IRFU, France; GNSF, Georgia; BMBF, DFG, HGF, MPG and AvH Foundation, Germany; GSRT, Greece; ISF, MINERVA, GIF, DIP and Benoziyo Center, Israel;

INFN, Italy; MEXT and JSPS, Japan; CNRST, Morocco; FOM and NWO, Netherlands; RCN, Norway; MNiSW, Poland; GRICES and FCT, Portugal; MERYS (MECTS), Romania; MES of Russia and ROSATOM, Russian Federation; JINR; MSTU, Serbia; MSSR, Slovakia; ARRS and MVZT, Slovenia; DST/NRF, South Africa; MICINN, Spain; SRC and Wallenberg Foundation, Sweden; SER, SNSF and Cantons of Bern and Geneva, Switzerland; NSC, Taiwan; TAEK, Turkey; STFC, the Royal Society and Leverhulme Trust, United Kingdom; DOE and NSF, United States of America.

The crucial computing support from all WLCG partners is acknowledged gratefully, in particular from CERN and the ATLAS Tier-1 facilities at TRIUMF (Canada), NDGF (Denmark, Norway, Sweden), CC-IN2P3 (France), KIT/GridKA (Germany), INFN-CNAF (Italy), NL-T1 (Netherlands), PIC (Spain), ASGC (Taiwan), RAL (UK) and BNL (USA) and in the Tier-2 facilities worldwide.

-
- [1] CMS Collaboration, Phys. Lett. B **716**, 30-61 (2012), [arXiv:hep-ex/1207.7235 \[hep-ex\]](#).
- [2] ATLAS Collaboration, Phys. Lett. B **716**, 1-29 (2012), [arXiv:hep-ex/1207.7214 \[hep-ex\]](#).
- [3] M. Montull and F. Riva, J. High Energy Phys. **11**, 018 (2012), [arXiv:hep-ph/1207.1716 \[hep-ph\]](#).
- [4] C. Degrande, J.-M. Gerard, C. Grojean, F. Maltoni, and G. Servant, J. High Energy Phys. **3**, 125 (2011), [arXiv:hep-ph/1010.6304 \[hep-ph\]](#).
- [5] H. Georgi, L. Kaplan, D. Morin, and A. Schenk, Phys. Rev. D **51**, 3888–3894 (1995).
- [6] A. Pomarol and J. Serra, Phys. Rev. D **78**, 074026 (2008), [arXiv:hep-ph/0806.3247 \[hep-ph\]](#).
- [7] B. Lillie, J. Shu, and T. M. Tait, J. High Energy Phys. **4**, 087 (2008), [arXiv:hep-ph/0712.3057 \[hep-ph\]](#).
- [8] K. Kumar, T. M. Tait, and R. Vega-Morales, J. High Energy Phys. **5**, 022 (2009), [arXiv:hep-ph/0901.3808 \[hep-ph\]](#).
- [9] M. Guchait, F. Mahmoudi, and K. Sridhar, Phys. Lett. B **666**, 347-351 (2008), [arXiv:hep-ph/0710.2234 \[hep-ph\]](#).
- [10] A. Bredenstein, A. Denner, S. Dittmaier, and S. Pozzorini, Phys. Rev. Lett. **103**, 012002 (2009), [arXiv:hep-ph/0905.0110 \[hep-ph\]](#).
- [11] ATLAS Collaboration, JINST **3**, S08003 (2008).
- [12] ATLAS uses a right-handed coordinate system with its origin at the nominal interaction point (IP) in the centre of the detector and the z -axis along the beam pipe. The x -axis points from the IP to the centre of the LHC ring, and the y -axis points upward. Cylindrical coordinates (r, ϕ) are used in the transverse plane, ϕ being the azimuthal angle around the beam pipe. The pseudorapidity is defined in terms of the polar angle θ as $\eta = -\text{Intan}(\theta/2)$. Transverse momentum and energy are defined as $p_T = p \sin \theta$ and $E_T = E \sin \theta$, respectively.
- [13] ATLAS Collaboration, New J. Phys. **13**, 053033 (2011), [arXiv:hep-ex/1012.5104 \[hep-ex\]](#).
- [14] M. L. Mangano, M. Moretti, F. Piccinini, R. Pittau, and A. D. Polosa, J. High Energy Phys. **7**, 001 (2003), [arXiv:hep-ph/0206293 \[hep-ph\]](#).
- [15] D. Stump et al., J. High Energy Phys. **10**, 046 (2003), [arXiv:hep-ph/0303013 \[hep-ph\]](#).
- [16] G. Corcella et al., J. High Energy Phys. **1**, 010 (2001), [arXiv:hep-ph/0011363 \[hep-ph\]](#).
- [17] $\Delta R = \sqrt{(\Delta\phi)^2 + (\Delta\eta)^2}$, where $\Delta\eta$ is the separation in η between the quark and jet and $\Delta\phi$ is the separation in ϕ .
- [18] J. M. Butterworth, J. R. Forshaw, and M. H. Seymour, Z. Phys. C **72**, 637-646 (1996), [arXiv:hep-ph/9601371 \[hep-ph\]](#).
- [19] ATLAS Collaboration, ATL-PHYS-PUB-2010-014, <http://cds.cern.ch/record/1300244>.
- [20] T. Sjöstrand, S. Mrenna, and P. Skands, J. High Energy Phys. **5**, 026 (2006), [arXiv:hep-ph/0603175 \[hep-ph\]](#).
- [21] H. L. Lai et al., Eur. Phys. J. C **12**, 375-392 (2000), [arXiv:hep-ph/9903282 \[hep-ph\]](#).
- [22] A. Martin, W. Stirling, R. Thorne, and G. Watt, Eur. Phys. J. C **63**, 189-285 (2009), [arXiv:hep-ph/0901.0002 \[hep-ph\]](#).
- [23] B. P. Kersevan and E. Richter-Was, Comput. Phys. Commun. **184**, 919-985 (2013).
- [24] P. Z. Skands, Phys. Rev. D **82**, 074018 (2010), [arXiv:hep-ph/1005.3457 \[hep-ph\]](#).
- [25] ATLAS Collaboration, Eur. Phys. J. C **72**, 2043 (2012), [arXiv:hep-ex/1203.5015 \[hep-ex\]](#).
- [26] M. Aliev et al., Comput. Phys. Commun. **182**, 1034-1046 (2011), [arXiv:hep-ph/1007.1327 \[hep-ph\]](#).
- [27] S. Frixione and B. R. Webber, J. High Energy Phys. **6**,

- 029 (2002), [arXiv:hep-ph/0204244 \[hep-ph\]](#).
- [28] S. Agostinelli et al., Nucl. Instrum Methods Phys. Res., Sect. A **506**, 250 (2003).
- [29] ATLAS Collaboration, Eur. Phys. J. C **70**, 823-874 (2010), [arXiv:hep-ex/1005.4568 \[hep-ex\]](#).
- [30] ATLAS Collaboration, Eur. Phys. J. C **72**, 1849 (2012), [arXiv:hep-ex/1110.1530 \[hep-ex\]](#).
- [31] ATLAS Collaboration, ATLAS-CONF-2012-099, <http://cds.cern.ch/record/1462601>.
- [32] ATLAS Collaboration, Eur. Phys. J. C **72**, 1909 (2012), [arXiv:hep-ex/1110.3174 \[hep-ex\]](#).
- [33] M. Cacciari, G. P. Salam, and G. Soyez, J. High Energy Phys. 4, 063 (2008), [arXiv:hep-ph/0802.1189 \[hep-ph\]](#).
- [34] ATLAS Collaboration, Eur. Phys. J. C **73**, 2304 (2013), [arXiv:hep-ex/1112.6426 \[hep-ex\]](#).
- [35] ATLAS Collaboration, ATLAS-CONF-2012-040, <https://cds.cern.ch/record/1435194>.
- [36] ATLAS Collaboration, ATLAS-CONF-2012-043, <http://cdsweb.cern.ch/record/1435197>.
- [37] ATLAS Collaboration, ATLAS-CONF-2012-039, <https://cds.cern.ch/record/1435193>.
- [38] S. Alioli, P. Nason, C. Oleari, and E. Re, J. High Energy Phys. 6, 043 (2010), [arXiv:hep-ph/1002.2581 \[hep-ph\]](#).
- [39] F. Maltoni and T. Stelzer, J. High Energy Phys. 2, 027 (2003), [arXiv:hep-ph/0208156 \[hep-ph\]](#).
- [40] ATLAS Collaboration, ATLAS-CONF-2010-099, <https://cds.cern.ch/record/1312145>.

The ATLAS Collaboration

G. Aad⁴⁸, T. Abajyan²¹, B. Abbott¹¹¹, J. Abdallah¹², S. Abdel Khalek¹¹⁵, A.A. Abdelalim⁴⁹, O. Abdinov¹¹, R. Aben¹⁰⁵, B. Abi¹¹², M. Abolins⁸⁸, O.S. AbouZeid¹⁵⁸, H. Abramowicz¹⁵³, H. Abreu¹³⁶, Y. Abulaiti^{146a,146b}, B.S. Acharya^{164a,164b,a}, L. Adamczyk^{38a}, D.L. Adams²⁵, T.N. Addy⁵⁶, J. Adelman¹⁷⁶, S. Adomeit⁹⁸, T. Adye¹²⁹, S. Aefsky²³, J.A. Aguilar-Saavedra^{124b,b}, M. Agustoni¹⁷, S.P. Ahlen²², F. Ahles⁴⁸, A. Ahmad¹⁴⁸, M. Ahsan⁴¹, G. Aielli^{133a,133b}, T.P.A. Åkesson⁷⁹, G. Akimoto¹⁵⁵, A.V. Akimov⁹⁴, M.A. Alam⁷⁶, J. Albert¹⁶⁹, S. Albrand⁵⁵, M. Aleksa³⁰, I.N. Aleksandrov⁶⁴, F. Alessandria^{89a}, C. Alexa^{26a}, G. Alexander¹⁵³, G. Alexandre⁴⁹, T. Alexopoulos¹⁰, M. Alhroob^{164a,164c}, M. Aliev¹⁶, G. Alimonti^{89a}, J. Alison³¹, B.M.M. Allbrooke¹⁸, L.J. Allison⁷¹, P.P. Allport⁷³, S.E. Allwood-Spiers⁵³, J. Almond⁸², A. Aloisio^{102a,102b}, R. Alon¹⁷², A. Alonso³⁶, F. Alonso⁷⁰, A. Altheimer³⁵, B. Alvarez Gonzalez⁸⁸, M.G. Alviggi^{102a,102b}, K. Amako⁶⁵, C. Amelung²³, V.V. Ammosov^{128,*}, S.P. Amor Dos Santos^{124a}, A. Amorim^{124a,c}, S. Amoroso⁴⁸, N. Amram¹⁵³, C. Anastopoulos³⁰, L.S. Ancu¹⁷, N. Andari³⁰, T. Andeen³⁵, C.F. Anders^{58b}, G. Anders^{58a}, K.J. Anderson³¹, A. Andreazza^{89a,89b}, V. Andrei^{58a}, X.S. Anduaga⁷⁰, S. Angelidakis⁹, P. Anger⁴⁴, A. Angerami³⁵, F. Anghinolfi³⁰, A. Anisenkov¹⁰⁷, N. Anjos^{124a}, A. Annovi⁴⁷, A. Antonaki⁹, M. Antonelli⁴⁷, A. Antonov⁹⁶, J. Antos^{144b}, F. Anulli^{132a}, M. Aoki¹⁰¹, L. Aperio Bella¹⁸, R. Apolle^{118,d}, G. Arabidze⁸⁸, I. Aracena¹⁴³, Y. Arai⁶⁵, A.T.H. Arce⁴⁵, S. Arfaoui¹⁴⁸, J-F. Arguin⁹³, S. Argyropoulos⁴², E. Arik^{19a,*}, M. Arik^{19a}, A.J. Armbruster⁸⁷, O. Arnaez⁸¹, V. Arnal⁸⁰, A. Artamonov⁹⁵, G. Artoni^{132a,132b}, D. Arutinov²¹, S. Asai¹⁵⁵, S. Ask²⁸, B. Åsman^{146a,146b}, L. Asquith⁶, K. Assamagan²⁵, R. Astalos^{144a}, A. Astbury¹⁶⁹, M. Atkinson¹⁶⁵, B. Auerbach⁶, E. Auge¹¹⁵, K. Augsten¹²⁶, M. Auroousseau^{145a}, G. Avolio³⁰, D. Axen¹⁶⁸, G. Azuelos^{93,e}, Y. Azuma¹⁵⁵, M.A. Baak³⁰, G. Baccaglioni^{89a}, C. Bacci^{134a,134b}, A.M. Bach¹⁵, H. Bachacou¹³⁶, K. Bachas¹⁵⁴, M. Backes⁴⁹, M. Backhaus²¹, J. Backus Mayes¹⁴³, E. Badescu^{26a}, P. Bagnaia^{132a,132b}, Y. Bai^{33a}, D.C. Bailey¹⁵⁸, T. Bain³⁵, J.T. Baines¹²⁹, O.K. Baker¹⁷⁶, S. Baker⁷⁷, P. Balek¹²⁷, F. Balli¹³⁶, E. Banas³⁹, P. Banerjee⁹³, Sw. Banerjee¹⁷³, D. Banfi³⁰, A. Bangert¹⁵⁰, V. Bansal¹⁶⁹, H.S. Bansil¹⁸, L. Barak¹⁷², S.P. Baranov⁹⁴, T. Barber⁴⁸, E.L. Barberio⁸⁶, D. Barberis^{50a,50b}, M. Barbero⁸³, D.Y. Bardin⁶⁴, T. Barillari⁹⁹, M. Barisonzi¹⁷⁵, T. Barklow¹⁴³, N. Barlow²⁸, B.M. Barnett¹²⁹, R.M. Barnett¹⁵, A. Baroncelli^{134a}, G. Barone⁴⁹, A.J. Barr¹¹⁸, F. Barreiro⁸⁰, J. Barreiro Guimarães da Costa⁵⁷, R. Bartoldus¹⁴³, A.E. Barton⁷¹, V. Bartsch¹⁴⁹, A. Basye¹⁶⁵, R.L. Bates⁵³, L. Batkova^{144a}, J.R. Batley²⁸, A. Battaglia¹⁷, M. Battistin³⁰, F. Bauer¹³⁶, H.S. Bawa^{143,f}, S. Beale⁹⁸, T. Beau⁷⁸, P.H. Beauchemin¹⁶¹, R. Beccherle^{50a}, P. Bechtel²¹, H.P. Beck¹⁷, K. Becker¹⁷⁵, S. Becker⁹⁸, M. Beckingham¹³⁸, K.H. Becks¹⁷⁵, A.J. Beddall^{19c}, A. Beddall^{19c}, S. Bedikian¹⁷⁶, V.A. Bednyakov⁶⁴, C.P. Bee⁸³, L.J. Beemster¹⁰⁵, T.A. Beermann¹⁷⁵, M. Beger²⁵, C. Belanger-Champagne⁸⁵, P.J. Bell⁴⁹, W.H. Bell⁴⁹, G. Bella¹⁵³, L. Bellagamba^{20a}, A. Bellerive²⁹, M. Bellomo³⁰, A. Belloni⁵⁷, O. Beloborodova^{107,g}, K. Belotskiy⁹⁶, O. Beltramello³⁰, O. Benary¹⁵³, D. Benckekroun^{135a}, K. Bendtz^{146a,146b}, N. Benekos¹⁶⁵, Y. Benhammou¹⁵³, E. Benhar Noccioni⁴⁹, J.A. Benitez Garcia^{159b}, D.P. Benjamin⁴⁵, J.R. Bensinger²³, K. Benslama¹³⁰, S. Bentvelsen¹⁰⁵, D. Berge³⁰, E. Bergeaas Kuutmann¹⁶, N. Berger⁵, F. Berghaus¹⁶⁹, E. Berglund¹⁰⁵, J. Beringer¹⁵, P. Bernat⁷⁷, R. Bernhard⁴⁸, C. Bernius²⁵, F.U. Bernlochner¹⁶⁹, T. Berry⁷⁶, C. Bertella⁸³, A. Bertin^{20a,20b}, F. Bertolucci^{122a,122b}, M.I. Besana^{89a,89b}, G.J. Besjes¹⁰⁴, N. Besson¹³⁶, S. Bethke⁹⁹, W. Bhimji⁴⁶, R.M. Bianchi³⁰, L. Bianchini²³, M. Bianco^{72a,72b}, O. Biebel⁹⁸, S.P. Bieniek⁷⁷, K. Bierwagen⁵⁴, J. Biesiada¹⁵, M. Biglietti^{134a}, H. Bilokon⁴⁷, M. Bindi¹¹⁵, S. Binet^{19c}, A. Bingul^{19c}, C. Bini^{132a,132b}, C. Biscarat¹⁷⁸, B. Bittner⁹⁹, C.W. Black¹⁵⁰, J.E. Black¹⁴³, K.M. Black²², R.E. Blair⁶, J.-B. Blanchard¹³⁶, T. Blazek^{144a}, I. Bloch⁴², C. Blocker²³, J. Blocki³⁹, W. Blum⁸¹, U. Blumenschein⁵⁴, G.J. Bobbink¹⁰⁵, V.S. Bobrovnikov¹⁰⁷, S.S. Bocchetta⁷⁹, A. Bocci⁴⁵, C.R. Boddy¹¹⁸, M. Boehler⁴⁸, J. Boek¹⁷⁵, T.T. Boek¹⁷⁵, N. Boelaert³⁶, J.A. Bogaerts³⁰, A. Bogdanov¹⁰⁷, A. Bogouch^{90,*}, C. Bohm^{146a}, J. Bohm¹²⁵, V. Boisvert⁷⁶, T. Bold^{38a}, V. Boldea^{26a}, N.M. Bolnet¹³⁶, M. Bomben⁷⁸, M. Bona⁷⁵, M. Boonekamp¹³⁶, S. Bordononi⁷⁸, C. Borer¹⁷, A. Borisov¹²⁸, G. Borissov⁷¹, I. Borjanovic^{13a}, M. Borri⁸², S. Borroni⁴², J. Bortfeldt⁹⁸, V. Bortolotto^{134a,134b}, K. Bos¹⁰⁵, D. Boscherini^{20a}, M. Bosman¹², H. Boterenbrood¹⁰⁵, J. Bouchami⁹³, J. Boudreau¹²³, E.V. Bouhova-Thacker⁷¹, D. Boumediene³⁴, C. Bourdarios¹¹⁵, N. Bousson⁸³, S. Boutouil^{135d}, A. Boveia³¹, J. Boyd³⁰, I.R. Boyko⁶⁴, I. Bozovic-Jelisavcic^{13b}, J. Bracinik¹⁸, P. Branchini^{134a}, A. Brandt⁸, G. Brandt¹¹⁸, O. Brandt⁵⁴, U. Bratzler¹⁵⁶, B. Brau⁸⁴, J.E. Brau¹¹⁴, H.M. Braun^{175,*}, S.F. Brazzale^{164a,164c}, B. Brelier¹⁵⁸, J. Bremer³⁰, K. Brendlinger¹²⁰, R. Brenner¹⁶⁶, S. Bressler¹⁷², T.M. Bristow^{145b}, D. Britton⁵³, F.M. Brochu²⁸, I. Brock²¹, R. Brock⁸⁸, F. Broggi^{89a}, C. Bromberg⁸⁸, J. Bronner⁹⁹, G. Brooijmans³⁵, T. Brooks⁷⁶, W.K. Brooks^{32b}, G. Brown⁸², P.A. Bruckman de Renstrom³⁹, D. Bruncko^{144b}, R. Bruneliere⁴⁸, S. Brunet⁶⁰, A. Bruni^{20a}, G. Bruni^{20a}, M. Bruschi^{20a}, L. Bryngemark⁷⁹, T. Buanes¹⁴, Q. Buat⁵⁵, F. Bucci⁴⁹, J. Buchanan¹¹⁸, P. Buchholz¹⁴¹, R.M. Buckingham¹¹⁸, A.G. Buckley⁴⁶, S.I. Buda^{26a}, I.A. Budagov⁶⁴, B. Budick¹⁰⁸, L. Bugge¹¹⁷, O. Bulekov⁹⁶, A.C. Bundock⁷³, M. Bunse⁴³, T. Buran^{117,*}, H. Burckhart³⁰, S. Burdini⁷³, T. Burgess¹⁴, S. Burke¹²⁹, E. Busato³⁴, V. Büscher⁸¹, P. Bussey⁵³, C.P. Buszello¹⁶⁶, B. Butler⁵⁷, J.M. Butler²², C.M. Buttar⁵³, J.M. Butterworth⁷⁷, W. Buttinger²⁸, M. Byszewski³⁰, S. Cabrera Urbán¹⁶⁷, D. Caforio^{20a,20b}, O. Cakir^{4a},

P. Calafiura¹⁵, G. Calderini⁷⁸, P. Calfayan⁹⁸, R. Calkins¹⁰⁶, L.P. Caloba^{24a}, R. Caloi^{132a,132b}, D. Calvet³⁴, S. Calvet³⁴, R. Camacho Toro⁴⁹, P. Camarri^{133a,133b}, D. Cameron¹¹⁷, L.M. Caminada¹⁵, R. Caminal Armadans¹², S. Campana³⁰, M. Campanelli⁷⁷, V. Canale^{102a,102b}, F. Canelli³¹, A. Canepa^{159a}, J. Cantero⁸⁰, R. Cantrill⁷⁶, T. Cao⁴⁰, M.D.M. Capeans Garrido³⁰, I. Caprini^{26a}, M. Caprini^{26a}, D. Capriotti⁹⁹, M. Capua^{37a,37b}, R. Caputo⁸¹, R. Cardarelli^{133a}, T. Carli³⁰, G. Carlino^{102a}, L. Carminati^{89a,89b}, S. Caron¹⁰⁴, E. Carquin^{32b}, G.D. Carrillo-Montoya^{145b}, A.A. Carter⁷⁵, J.R. Carter²⁸, J. Carvalho^{124a,h}, D. Casadei¹⁰⁸, M.P. Casado¹², M. Cascella^{122a,122b}, C. Caso^{50a,50b,*}, E. Castaneda-Miranda¹⁷³, A. Castelli¹⁰⁵, V. Castillo Gimenez¹⁶⁷, N.F. Castro^{124a}, G. Cataldi^{72a}, P. Catastini⁵⁷, A. Catinaccio³⁰, J.R. Catmore³⁰, A. Cattai³⁰, G. Cattani^{133a,133b}, S. Caughron⁸⁸, V. Cavaliere¹⁶⁵, P. Cavalleri⁷⁸, D. Cavalli^{89a}, M. Cavalli-Sforza¹², V. Cavasinni^{122a,122b}, F. Ceradini^{134a,134b}, B. Cerio⁴⁵, A.S. Cerqueira^{24b}, A. Cerri¹⁵, L. Cerrito⁷⁵, F. Cerutti¹⁵, A. Cervelli¹⁷, S.A. Cetin^{19b}, A. Chafaq^{135a}, D. Chakraborty¹⁰⁶, I. Chalupkova¹²⁷, K. Chan³, P. Chang¹⁶⁵, B. Chapleau⁸⁵, J.D. Chapman²⁸, J.W. Chapman⁸⁷, D.G. Charlton¹⁸, V. Chavda⁸², C.A. Chavez Barajas³⁰, S. Cheatham⁸⁵, S. Chekanov⁶, S.V. Chekulaev^{159a}, G.A. Chelkov⁶⁴, M.A. Chelstowska¹⁰⁴, C. Chen⁶³, H. Chen²⁵, S. Chen^{33c}, X. Chen¹⁷³, Y. Chen³⁵, Y. Cheng³¹, A. Cheplakov⁶⁴, R. Cherkaoui El Moursli^{135e}, V. Chernyatin²⁵, E. Cheu⁷, S.L. Cheung¹⁵⁸, L. Chevalier¹³⁶, G. Chiefari^{102a,102b}, L. Chikovani^{51a,*}, J.T. Childers³⁰, A. Chilingarov⁷¹, G. Chiodini^{72a}, A.S. Chisholm¹⁸, R.T. Chislett⁷⁷, A. Chitan^{26a}, M.V. Chizhov⁶⁴, G. Choudalakis³¹, S. Chouridou⁹, B.K.B. Chow⁹⁸, I.A. Christidi⁷⁷, A. Christov⁴⁸, D. Chromek-Burckhart³⁰, M.L. Chu¹⁵¹, J. Chudoba¹²⁵, G. Ciapetti^{132a,132b}, A.K. Ciftci^{4a}, R. Ciftci^{4a}, D. Cinca⁶², V. Cindro⁷⁴, A. Ciocio¹⁵, M. Cirilli⁸⁷, P. Cirkovic^{13b}, Z.H. Citron¹⁷², M. Citterio^{89a}, M. Ciubancan^{26a}, A. Clark⁴⁹, P.J. Clark⁴⁶, R.N. Clarke¹⁵, J.C. Clemens⁸³, B. Clement⁵⁵, C. Clement^{146a,146b}, Y. Coadou⁸³, M. Cobal^{164a,164c}, A. Coccaro¹³⁸, J. Cochran⁶³, L. Coffey²³, J.G. Cogan¹⁴³, J. Coggeshall¹⁶⁵, J. Colas⁵, S. Cole¹⁰⁶, A.P. Colijn¹⁰⁵, N.J. Collins¹⁸, C. Collins-Tooth⁵³, J. Collot⁵⁵, T. Colombo^{119a,119b}, G. Colon⁸⁴, G. Compostella⁹⁹, P. Conde Muiño^{124a}, E. Coniavitis¹⁶⁶, M.C. Conidi¹², S.M. Consonni^{89a,89b}, V. Consorti⁴⁸, S. Constantinescu^{26a}, C. Conta^{119a,119b}, G. Conti⁵⁷, F. Conventi^{102a,i}, M. Cooke¹⁵, B.D. Cooper⁷⁷, A.M. Cooper-Sarkar¹¹⁸, N.J. Cooper-Smith⁷⁶, K. Copic¹⁵, T. Cornelissen¹⁷⁵, M. Corradi^{20a}, F. Corriveau^{85,j}, A. Corso-Radu¹⁶³, A. Cortes-Gonzalez¹⁶⁵, G. Cortiana⁹⁹, G. Costa^{89a}, M.J. Costa¹⁶⁷, D. Costanzo¹³⁹, D. Côté³⁰, G. Cottin^{32a}, L. Courneyea¹⁶⁹, G. Cowan⁷⁶, B.E. Cox⁸², K. Cranmer¹⁰⁸, S. Crépe-Renaudin⁵⁵, F. Crescioli⁷⁸, M. Cristinziani²¹, G. Crosetti^{37a,37b}, C.-M. Cuciu^{26a}, C. Cuenca Almenar¹⁷⁶, T. Cuhadar Donszelmann¹³⁹, J. Cummings¹⁷⁶, M. Curatolo⁴⁷, C.J. Curtis¹⁸, C. Cuthbert¹⁵⁰, H. Czirr¹⁴¹, P. Czodrowski⁴⁴, Z. Czyczula¹⁷⁶, S. D'Auria⁵³, M. D'Onofrio⁷³, A. D'Orazio^{132a,132b}, M.J. Da Cunha Sargedas De Sousa^{124a}, C. Da Via⁸², W. Dabrowski^{38a}, A. Dafinca¹¹⁸, T. Dai⁸⁷, F. Dallaire⁹³, C. Dallapiccola⁸⁴, M. Dam³⁶, D.S. Damiani¹³⁷, A.C. Daniells¹⁸, H.O. Danielsson³⁰, V. Dao¹⁰⁴, G. Darbo^{50a}, G.L. Darlea^{26b}, S. Darmora⁸, J.A. Dassoulas⁴², W. Davey²¹, T. Davidek¹²⁷, N. Davidson⁸⁶, E. Davies^{118,d}, M. Davies⁹³, O. Davignon⁷⁸, A.R. Davison⁷⁷, Y. Davygora^{58a}, E. Dawe¹⁴², I. Dawson¹³⁹, R.K. Daya-Ishmukhametova²³, K. De⁸, R. de Asmundis^{102a}, S. De Castro^{20a,20b}, S. De Cecco⁷⁸, J. de Graat⁹⁸, N. De Groot¹⁰⁴, P. de Jong¹⁰⁵, C. De La Taille¹¹⁵, H. De la Torre⁸⁰, F. De Lorenzi⁶³, L. De Nooij¹⁰⁵, D. De Pedis^{132a}, A. De Salvo^{132a}, U. De Sanctis^{164a,164c}, A. De Santo¹⁴⁹, J.B. De Vivie De Regie¹¹⁵, G. De Zorzi^{132a,132b}, W.J. Dearnaley⁷¹, R. Debbe²⁵, C. Debenedetti⁴⁶, B. Dechenaux⁵⁵, D.V. Dedovich⁶⁴, J. Degenhardt¹²⁰, J. Del Peso⁸⁰, T. Del Prete^{122a,122b}, T. Delemontex⁵⁵, M. Deliyergiyev⁷⁴, A. Dell'Acqua³⁰, L. Dell'Asta²², M. Della Pietra^{102a,i}, D. della Volpe^{102a,102b}, M. Delmastro⁵, P.A. Delsart⁵⁵, C. Deluca¹⁰⁵, S. Demers¹⁷⁶, M. Demichev⁶⁴, B. Demirkoz^{12,k}, S.P. Denisov¹²⁸, D. Derendarz³⁹, J.E. Derkaoui^{135d}, F. Derue⁷⁸, P. Dervan⁷³, K. Desch²¹, P.O. Deviveiros¹⁰⁵, A. Dewhurst¹²⁹, B. DeWilde¹⁴⁸, S. Dhaliwal¹⁰⁵, R. Dhullipudi^{25,l}, A. Di Ciaccio^{133a,133b}, L. Di Ciaccio⁵, C. Di Donato^{102a,102b}, A. Di Girolamo³⁰, B. Di Girolamo³⁰, S. Di Luise^{134a,134b}, A. Di Mattia¹⁵², B. Di Micco³⁰, R. Di Nardo⁴⁷, A. Di Simone^{133a,133b}, R. Di Sipio^{20a,20b}, M.A. Diaz^{32a}, E.B. Diehl⁸⁷, J. Dietrich⁴², T.A. Dietzsch^{58a}, S. Diglio⁸⁶, K. Dindar Yagci⁴⁰, J. Dingfelder²¹, F. Dinut^{26a}, C. Dionisi^{132a,132b}, P. Dita^{26a}, S. Dita^{26a}, F. Dittus³⁰, F. Djama⁸³, T. Djobava^{51b}, M.A.B. do Vale^{24c}, A. Do Valle Wemans^{124a,m}, T.K.O. Doan⁵, D. Dobos³⁰, E. Dobson⁷⁷, J. Dodd³⁵, C. Doglioni⁴⁹, T. Doherty⁵³, T. Dohmae¹⁵⁵, Y. Doi^{65,*}, J. Dolejsi¹²⁷, Z. Dolezal¹²⁷, B.A. Dolgoshein^{96,*}, M. Donadelli^{24d}, J. Donini³⁴, J. Dopke³⁰, A. Doria^{102a}, A. Dos Anjos¹⁷³, A. Dotti^{122a,122b}, M.T. Dova⁷⁰, A.T. Doyle⁵³, N. Dressnandt¹²⁰, M. Dris¹⁰, J. Dubbert⁸⁷, S. Dube¹⁵, E. Dubreuil³⁴, E. Duchovni¹⁷², G. Duckeck⁹⁸, D. Duda¹⁷⁵, A. Dudarev³⁰, F. Dudziak⁶³, I.P. Duerdoth⁸², L. Duflot¹¹⁵, M.-A. Dufour⁸⁵, L. Duguid⁷⁶, M. Dührssen³⁰, M. Dunford^{58a}, H. Duran Yildiz^{4a}, M. Düren⁵², R. Duxfield¹³⁹, M. Dwuznik^{38a}, W.L. Ebenstein⁴⁵, J. Ebke⁹⁸, S. Eckweiler⁸¹, W. Edson², C.A. Edwards⁷⁶, N.C. Edwards⁵³, W. Ehrenfeld²¹, T. Eifert¹⁴³, G. Eigen¹⁴, K. Ellis⁷⁵, N. Ellis³⁰, J. Elmsheuser⁹⁸, M. Elsing³⁰, D. Emelianov¹²⁹, Y. Enari¹⁵⁵, R. Engelmann¹⁴⁸, A. Engl⁹⁸, B. Epp⁶¹, J. Erdmann¹⁷⁶, A. Ereditato¹⁷, D. Eriksson^{146a}, J. Ernst², M. Ernst²⁵, J. Ernwein¹³⁶, D. Errede¹⁶⁵, S. Errede¹⁶⁵, E. Ertel⁸¹, M. Escalier¹¹⁵, H. Esch⁴³, C. Escobar¹²³, X. Espinal Curull¹², B. Esposito⁴⁷, F. Etienne⁸³, A.I. Etievre¹³⁶, E. Etzion¹⁵³, D. Evangelakou⁵⁴, H. Evans⁶⁰,

L. Fabbri^{20a,20b}, C. Fabre³⁰, G. Facini³⁰, R.M. Fakhruddinov¹²⁸, S. Falciano^{132a}, Y. Fang^{33a}, M. Fanti^{89a,89b}, A. Farbin⁸, A. Farilla^{134a}, J. Farley¹⁴⁸, T. Farooque¹⁵⁸, S. Farrell¹⁶³, S.M. Farrington¹⁷⁰, P. Farthouat³⁰, F. Fassi¹⁶⁷, P. Fassnacht³⁰, D. Fassouliotis⁹, B. Fatholahzadeh¹⁵⁸, A. Favaretto^{89a,89b}, L. Fayard¹¹⁵, P. Federic^{144a}, O.L. Fedin¹²¹, W. Fedorko¹⁶⁸, M. Fehling-Kaschek⁴⁸, L. Feligioni⁸³, C. Feng^{33d}, E.J. Feng⁶, H. Feng⁸⁷, A.B. Fenyuk¹²⁸, J. Ferencei^{144b}, W. Fernando⁶, S. Ferrag⁵³, J. Ferrando⁵³, V. Ferrara⁴², A. Ferrari¹⁶⁶, P. Ferrari¹⁰⁵, R. Ferrari^{119a}, D.E. Ferreira de Lima⁵³, A. Ferrer¹⁶⁷, D. Ferrere⁴⁹, C. Ferretti⁸⁷, A. Ferretto Parodi^{50a,50b}, M. Fiascaris³¹, F. Fiedler⁸¹, A. Filipčić⁷⁴, F. Filthaut¹⁰⁴, M. Fincke-Keeler¹⁶⁹, K.D. Finelli⁴⁵, M.C.N. Fiolhais^{124a,h}, L. Fiorini¹⁶⁷, A. Firan⁴⁰, J. Fischer¹⁷⁵, M.J. Fisher¹⁰⁹, E.A. Fitzgerald²³, M. Flechl⁴⁸, I. Fleck¹⁴¹, P. Fleischmann¹⁷⁴, S. Fleischmann¹⁷⁵, G.T. Fletcher¹³⁹, G. Fletcher⁷⁵, T. Flick¹⁷⁵, A. Floderus⁷⁹, L.R. Flores Castillo¹⁷³, A.C. Florez Bustos^{159b}, M.J. Flowerdew⁹⁹, T. Fonseca Martin¹⁷, A. Formica¹³⁶, A. Forti⁸², D. Fortin^{159a}, D. Fournier¹¹⁵, A.J. Fowler⁴⁵, H. Fox⁷¹, P. Francavilla¹², M. Franchini^{20a,20b}, S. Franchino³⁰, D. Francis³⁰, M. Franklin⁵⁷, S. Franz³⁰, M. Fraternali^{119a,119b}, S. Fratina¹²⁰, S.T. French²⁸, C. Friedrich⁴², F. Friedrich⁴⁴, D. Froidevaux³⁰, J.A. Frost²⁸, C. Fukunaga¹⁵⁶, E. Fullana Torregrosa¹²⁷, B.G. Fulson¹⁴³, J. Fuster¹⁶⁷, C. Gabaldon³⁰, O. Gabizon¹⁷², A. Gabrielli^{132a,132b}, S. Gadatsch¹⁰⁵, T. Gadfort²⁵, S. Gadowski⁴⁹, G. Gagliardi^{50a,50b}, P. Gagnon⁶⁰, C. Galea⁹⁸, B. Galhardo^{124a}, E.J. Gallas¹¹⁸, V. Gallo¹⁷, B.J. Gallop¹²⁹, P. Gallus¹²⁶, K.K. Gan¹⁰⁹, R.P. Gandrajula⁶², Y.S. Gao^{143,f}, A. Gaponenko¹⁵, F.M. Garay Walls⁴⁶, F. Garberson¹⁷⁶, C. García¹⁶⁷, J.E. García Navarro¹⁶⁷, M. Garcia-Sciveres¹⁵, R.W. Gardner³¹, N. Garelli¹⁴³, V. Garonne³⁰, C. Gatti⁴⁷, G. Gaudio^{119a}, B. Gaur¹⁴¹, L. Gauthier⁹³, P. Gauzzi^{132a,132b}, I.L. Gavrilenko⁹⁴, C. Gay¹⁶⁸, G. Gaycken²¹, E.N. Gazis¹⁰, P. Ge^{33d,n}, Z. Gecse¹⁶⁸, C.N.P. Gee¹²⁹, D.A.A. Geerts¹⁰⁵, Ch. Geich-Gimbel²¹, K. Gellerstedt^{146a,146b}, C. Gemme^{50a}, A. Gemmel⁵³, M.H. Genest⁵⁵, S. Gentile^{132a,132b}, M. George⁵⁴, S. George⁷⁶, D. Gerbaudo¹⁶³, P. Gerlach¹⁷⁵, A. Gershon¹⁵³, C. Geweniger^{58a}, H. Ghazlane^{135b}, N. Ghodbane³⁴, B. Giacobbe^{20a}, S. Giagu^{132a,132b}, V. Giangiobbe¹², F. Gianotti³⁰, B. Gibbard²⁵, A. Gibson¹⁵⁸, S.M. Gibson³⁰, M. Gilchriese¹⁵, T.P.S. Gillam²⁸, D. Gillberg³⁰, A.R. Gillman¹²⁹, D.M. Gingrich^{3,e}, N. Giokaris⁹, M.P. Giordani^{165a,164c}, R. Giordano^{102a,102b}, F.M. Giorgi¹⁶, P. Giovannini⁹⁹, P.F. Giraud¹³⁶, D. Giugni^{89a}, C. Giuliani⁴⁸, M. Giunta⁹³, B.K. Gjelsten¹¹⁷, L.K. Gladilin⁹⁷, C. Glasman⁸⁰, J. Glatzer²¹, A. Glazov⁴², G.L. Glonti⁶⁴, J.R. Goddard⁷⁵, J. Godfrey¹⁴², J. Godlewski³⁰, M. Goebel⁴², C. Goeringer⁸¹, S. Goldfarb⁸⁷, T. Golling¹⁷⁶, D. Golubkov¹²⁸, A. Gomes^{124a,c}, L.S. Gomez Fajardo⁴², R. Gonçalves⁷⁶, J. Goncalves Pinto Firmino Da Costa⁴², L. Gonella²¹, S. González de la Hoz¹⁶⁷, G. Gonzalez Parra¹², M.L. Gonzalez Silva²⁷, S. Gonzalez-Sevilla⁴⁹, J.J. Goodson¹⁴⁸, L. Goossens³⁰, T. Göpfert⁴⁴, P.A. Gorbounov⁹⁵, H.A. Gordon²⁵, I. Gorelov¹⁰³, G. Gorfine¹⁷⁵, B. Gorini³⁰, E. Gorini^{72a,72b}, A. Gorišek⁷⁴, E. Gornicki³⁹, A.T. Goshaw⁶, C. Gössling⁴³, M.I. Gostkin⁶⁴, I. Gough Eschrich¹⁶³, M. Gouighri^{135a}, D. Goujdami^{135c}, M.P. Goulette⁴⁹, A.G. Goussiou¹³⁸, C. Goy⁵, S. Gozpinar²³, L. Graber⁵⁴, I. Grabowska-Bold^{38a}, P. Grafström^{20a,20b}, K.-J. Grahm⁴², E. Gramstad¹¹⁷, F. Grancagnolo^{72a}, S. Grancagnolo¹⁶, V. Grassi¹⁴⁸, V. Gratchev¹²¹, H.M. Gray³⁰, J.A. Gray¹⁴⁸, E. Graziani^{134a}, O.G. Grebenyuk¹²¹, T. Greenshaw⁷³, Z.D. Greenwood^{25,i}, K. Gregersen³⁶, I.M. Gregor⁴², P. Grenier¹⁴³, J. Griffiths⁸, N. Grigalashvili⁶⁴, A.A. Grillo¹³⁷, K. Grimm⁷¹, S. Grinstein¹², Ph. Gris³⁴, Y.V. Grishkevich⁹⁷, J.-F. Grivaz¹¹⁵, J.P. Grohs⁴⁴, A. Grohsjean⁴², E. Gross¹⁷², J. Grosse-Knetter⁵⁴, J. Groth-Jensen¹⁷², K. Grybel¹⁴¹, D. Guest¹⁷⁶, O. Gueta¹⁵³, C. Guicheney³⁴, E. Guido^{50a,50b}, T. Guillemin¹¹⁵, S. Guindon⁵⁴, U. Gul⁵³, J. Gunther¹²⁶, B. Guo¹⁵⁸, J. Guo³⁵, P. Gutierrez¹¹¹, N. Guttman¹⁵³, O. Gutzwiller¹⁷³, C. Guyot¹³⁶, C. Gwenlan¹¹⁸, C.B. Gwilliam⁷³, A. Haas¹⁰⁸, S. Haas³⁰, C. Haber¹⁵, H.K. Hadavand⁸, P. Haefner²¹, Z. Hajduk³⁹, H. Hakobyan¹⁷⁷, D. Hall¹¹⁸, G. Halladjian⁶², K. Hamacher¹⁷⁵, P. Hamal¹¹³, K. Hamano⁸⁶, M. Hamer⁵⁴, A. Hamilton^{145b,o}, S. Hamilton¹⁶¹, L. Han^{33b}, K. Hanagaki¹¹⁶, K. Hanawa¹⁶⁰, M. Hance¹⁵, C. Handel⁸¹, P. Hanke^{58a}, J.R. Hansen³⁶, J.B. Hansen³⁶, J.D. Hansen³⁶, P.H. Hansen³⁶, P. Hansson¹⁴³, K. Hara¹⁶⁰, A.S. Hard¹⁷³, T. Harenberg¹⁷⁵, S. Harkusha⁹⁰, D. Harper⁸⁷, R.D. Harrington⁴⁶, O.M. Harris¹³⁸, J. Hartert⁴⁸, F. Hartjes¹⁰⁵, T. Haruyama⁶⁵, A. Harvey⁵⁶, S. Hasegawa¹⁰¹, Y. Hasegawa¹⁴⁰, S. Hassani¹³⁶, S. Haug¹⁷, M. Hauschild³⁰, R. Hauser⁸⁸, M. Havranek²¹, C.M. Hawkes¹⁸, R.J. Hawkins³⁰, A.D. Hawkins⁷⁹, T. Hayakawa⁶⁶, T. Hayashi¹⁶⁰, D. Hayden⁷⁶, C.P. Hays¹¹⁸, H.S. Hayward⁷³, S.J. Haywood¹²⁹, S.J. Head¹⁸, T. Heck⁸¹, V. Hedberg⁷⁹, L. Heelan⁸, S. Heim¹²⁰, B. Heinemann¹⁵, S. Heisterkamp³⁶, L. Helary²², C. Heller⁹⁸, M. Heller³⁰, S. Hellman^{146a,146b}, D. Hellmich²¹, C. Hensels¹², J. Henderson¹¹⁸, R.C.W. Henderson⁷¹, M. Henke^{58a}, A. Henrichs¹⁷⁶, A.M. Henriques Correia³⁰, S. Henrot-Versille¹¹⁵, C. Hensel⁵⁴, G.H. Herbert¹⁶, C.M. Hernandez⁸, Y. Hernández Jiménez¹⁶⁷, R. Herrberg¹⁶, G. Herten⁴⁸, R. Hertenberger⁹⁸, L. Hervas³⁰, G.G. Hesketh⁷⁷, N.P. Hessey¹⁰⁵, R. Hickling⁷⁵, E. Higón-Rodríguez¹⁶⁷, J.C. Hill²⁸, K.H. Hiller⁴², S. Hillert²¹, S.J. Hillier¹⁸, I. Hinchliffe¹⁵, E. Hines¹²⁰, M. Hirose¹¹⁶, D. Hirschbuehl¹⁷⁵, J. Hobbs¹⁴⁸, N. Hod¹⁰⁵, M.C. Hodgkinson¹³⁹, P. Hodgson¹³⁹, A. Hoecker³⁰, M.R. Hoefkamp¹⁰³, J. Hoffman⁴⁰, D. Hoffmann⁸³, J.I. Hofmann^{58a}, M. Hohlfield⁸¹, S.O. Holmgren^{146a}, J.L. Holzbauer⁸⁸, T.M. Hong¹²⁰, L. Hooft van Huysduynen¹⁰⁸, J.-Y. Hostachy⁵⁵, S. Hou¹⁵¹, A. Hoummada^{135a}, J. Howard¹¹⁸, J. Howarth⁸², M. Hrabovsky¹¹³, I. Hristova¹⁶, J. Hrivnac¹¹⁵, T. Hryn'ova⁵, P.J. Hsu⁸¹, S.-C. Hsu¹³⁸, D. Hu³⁵, Z. Hubacek³⁰, F. Hubaut⁸³, F. Huegging²¹, A. Huettmann⁴², T.B. Huffman¹¹⁸, E.W. Hughes³⁵,

G. Hughes⁷¹, M. Huhtinen³⁰, T.A. Hülsing⁸¹, M. Hurwitz¹⁵, N. Huseynov^{64,p}, J. Huston⁸⁸, J. Huth⁵⁷, G. Iacobucci⁴⁹, G. Iakovidis¹⁰, M. Ibbotson⁸², I. Ibragimov¹⁴¹, L. Iconomidou-Fayard¹¹⁵, J. Idarraga¹¹⁵, P. Iengo^{102a}, O. Igonkina¹⁰⁵, Y. Ikegami⁶⁵, K. Ikematsu¹⁴¹, M. Ikeno⁶⁵, D. Iliadis¹⁵⁴, N. Ilic¹⁵⁸, T. Ince⁹⁹, P. Ioannou⁹, M. Iodice^{134a}, K. Iordanidou⁹, V. Ippolito^{132a,132b}, A. Irlles Quiles¹⁶⁷, C. Isaksson¹⁶⁶, M. Ishino⁶⁷, M. Ishitsuka¹⁵⁷, R. Ishmukhametov¹⁰⁹, C. Issever¹¹⁸, S. Istin^{19a}, A.V. Ivashin¹²⁸, W. Iwanski³⁹, H. Iwasaki⁶⁵, J.M. Izen⁴¹, V. Izzo^{102a}, B. Jackson¹²⁰, J.N. Jackson⁷³, P. Jackson¹, M.R. Jaekel³⁰, V. Jain², K. Jakobs⁴⁸, S. Jakobsen³⁶, T. Jakoubek¹²⁵, J. Jakubek¹²⁶, D.O. Jamin¹⁵¹, D.K. Jana¹¹¹, E. Jansen⁷⁷, H. Jansen³⁰, J. Janssen²¹, A. Jantsch⁹⁹, M. Janus⁴⁸, R.C. Jared¹⁷³, G. Jarlskog⁷⁹, L. Jeanty⁵⁷, G.-Y. Jeng¹⁵⁰, I. Jen-La Plante³¹, D. Jennens⁸⁶, P. Jenni³⁰, C. Jeske¹⁷⁰, P. Jež³⁶, S. Jézéquel⁵, M.K. Jha^{20a}, H. Ji¹⁷³, W. Ji⁸¹, J. Jia¹⁴⁸, Y. Jiang^{33b}, M. Jimenez Belenguier⁴², S. Jin^{33a}, O. Jinnouchi¹⁵⁷, M.D. Joergensen³⁶, D. Joffe⁴⁰, M. Johansen^{146a,146b}, K.E. Johansson^{146a}, P. Johansson¹³⁹, S. Johnert⁴², K.A. Johns⁷, K. Jon-And^{146a,146b}, G. Jones¹⁷⁰, R.W.L. Jones⁷¹, T.J. Jones⁷³, C. Joram³⁰, P.M. Jorge^{124a}, K.D. Joshi⁸², J. Jovicevic¹⁴⁷, T. Jovin^{13b}, X. Ju¹⁷³, C.A. Jung⁴³, R.M. Jungst³⁰, P. Juscel⁶¹, A. Juste Rozas¹², S. Kabana¹⁷, M. Kaci¹⁶⁷, A. Kaczmarska³⁹, P. Kadlecik³⁶, M. Kado¹¹⁵, H. Kagan¹⁰⁹, M. Kagan⁵⁷, E. Kajomovitz¹⁵², S. Kalinin¹⁷⁵, S. Kama⁴⁰, N. Kanaya¹⁵⁵, M. Kaneda³⁰, S. Kaneti²⁸, T. Kanno¹⁵⁷, V.A. Kantserov⁹⁶, J. Kanzaki⁶⁵, B. Kaplan¹⁰⁸, A. Kapliy³¹, D. Kar⁵³, M. Karagounis²¹, K. Karakostas¹⁰, M. Karnevskiy⁸¹, V. Kartvelishvili⁷¹, A.N. Karyukhin¹²⁸, L. Kashif¹⁷³, G. Kasieczka^{58b}, R.D. Kass¹⁰⁹, A. Kastanas¹⁴, Y. Kataoka¹⁵⁵, J. Katzy⁴², V. Kaushik⁷, K. Kawagoe⁶⁹, T. Kawamoto¹⁵⁵, G. Kawamura⁵⁴, S. Kazama¹⁵⁵, V.F. Kazanin¹⁰⁷, M.Y. Kazarinov⁶⁴, R. Keeler¹⁶⁹, P.T. Keener¹²⁰, R. Kehoe⁴⁰, M. Keil⁵⁴, J.S. Keller¹³⁸, H. Keoshkerian⁵, O. Kepka¹²⁵, B.P. Kerševan⁷⁴, S. Kersten¹⁷⁵, K. Kessoku¹⁵⁵, J. Keung¹⁵⁸, F. Khalil-zada¹¹, H. Khandanyan^{146a,146b}, A. Khanov¹¹², D. Kharchenko⁶⁴, A. Khodinov⁹⁶, A. Khomich^{58a}, T.J. Khoo²⁸, G. Khorauli²¹, A. Khoroshilov¹⁷⁵, V. Khovanskiy⁹⁵, E. Khramov⁶⁴, J. Khubua^{51b}, H. Kim^{146a,146b}, S.H. Kim¹⁶⁰, N. Kimura¹⁷¹, O. Kind¹⁶, B.T. King⁷³, M. King⁶⁶, R.S.B. King¹¹⁸, S.B. King¹⁶⁸, J. Kirk¹²⁹, A.E. Kiryunin⁹⁹, T. Kishimoto⁶⁶, D. Kisielewska^{38a}, T. Kitamura⁶⁰, T. Kittelmann¹²³, K. Kiuchi¹⁶⁰, E. Kladiva^{144b}, M. Klein⁷³, U. Klein⁷³, K. Kleinknecht⁸¹, M. Klemetti⁸⁵, A. Klier¹⁷², P. Klimek^{146a,146b}, A. Klimentov²⁵, R. Klingenberg⁴³, J.A. Klinger⁸², E.B. Klinkby³⁶, T. Klioutchnikova³⁰, P.F. Klok¹⁰⁴, S. Klous¹⁰⁵, E.-E. Kluge^{58a}, P. Kluit¹⁰⁵, S. Kluth⁹⁹, E. Kneringer⁶¹, E.B.F.G. Knoops⁸³, A. Knue⁵⁴, B.R. Ko⁴⁵, T. Kobayashi¹⁵⁵, M. Kobel⁴⁴, M. Kocian¹⁴³, P. Kodys¹²⁷, S. Koenig⁸¹, F. Koetsveld¹⁰⁴, P. Koevesarki²¹, T. Koffas²⁹, E. Koffeman¹⁰⁵, L.A. Kogan¹¹⁸, S. Kohlmann¹⁷⁵, F. Kohn⁵⁴, Z. Kohout¹²⁶, T. Kohriki⁶⁵, T. Koi¹⁴³, H. Kolanoski¹⁶, I. Koletsou^{89a}, J. Koll⁸⁸, A.A. Komar⁹⁴, Y. Komori¹⁵⁵, T. Kondo⁶⁵, K. Köneke³⁰, A.C. König¹⁰⁴, T. Kono^{42,q}, A.I. Kononov⁴⁸, R. Konoplich^{108,r}, N. Konstantinidis⁷⁷, R. Kopeliansky¹⁵², S. Koperny^{38a}, L. Köpke⁸¹, A.K. Kopp⁴⁸, K. Korcyl³⁹, K. Kordas¹⁵⁴, A. Korn⁴⁶, A. Korol¹⁰⁷, I. Korolkov¹², E.V. Korolkova¹³⁹, V.A. Korotkov¹²⁸, O. Kortner⁹⁹, S. Kortner⁹⁹, V.V. Kostyukhin²¹, S. Kotov⁹⁹, V.M. Kotov⁶⁴, A. Kotwal⁴⁵, C. Kourkoumelis⁹, V. Kouskoura¹⁵⁴, A. Koutsman^{159a}, R. Kowalewski¹⁶⁹, T.Z. Kowalski^{38a}, W. Kozanecki¹³⁶, A.S. Kozhin¹²⁸, V. Kral¹²⁶, V.A. Kramarenko⁹⁷, G. Kramberger⁷⁴, M.W. Krasny⁷⁸, A. Krasznahorkay¹⁰⁸, J.K. Kraus²¹, A. Kravchenko²⁵, S. Kreiss¹⁰⁸, J. Kretzschmar⁷³, K. Kreutzfeldt⁵², N. Krieger⁵⁴, P. Krieger¹⁵⁸, K. Kroeninger⁵⁴, H. Kroha⁹⁹, J. Kroll¹²⁰, J. Kröseberg²¹, J. Krstic^{13a}, U. Kruchonak⁶⁴, H. Krüger²¹, T. Kruker¹⁷, N. Krumnack⁶³, Z.V. Krumshteyn⁶⁴, M.K. Kruse⁴⁵, T. Kubota⁸⁶, S. Kuday^{4a}, S. Kuehn⁴⁸, A. Kugel^{58c}, T. Kuhl⁴², V. Kukhtin⁶⁴, Y. Kulchitsky⁹⁰, S. Kuleshov^{32b}, M. Kuna⁷⁸, J. Kunkle¹²⁰, A. Kupco¹²⁵, H. Kurashige⁶⁶, M. Kurata¹⁶⁰, Y.A. Kurochkin⁹⁰, V. Kus¹²⁵, E.S. Kuwertz¹⁴⁷, M. Kuze¹⁵⁷, J. Kvita¹⁴², R. Kwee¹⁶, A. La Rosa⁴⁹, L. La Rotonda^{37a,37b}, L. Labarga⁸⁰, S. Lablak^{135a}, C. Lacasta¹⁶⁷, F. Lacava^{132a,132b}, J. Lacey²⁹, H. Lacker¹⁶, D. Lacour⁷⁸, V.R. Lacuesta¹⁶⁷, E. Ladygin⁶⁴, R. Lafaye⁵, B. Laforge⁷⁸, T. Lagouri¹⁷⁶, S. Lai⁴⁸, H. Laier^{58a}, E. Laisne⁵⁵, L. Lambourne⁷⁷, C.L. Lampen⁷, W. Lampl⁷, E. Lançon¹³⁶, U. Landgraf⁴⁸, M.P.J. Landon⁷⁵, V.S. Lang^{58a}, C. Lange⁴², A.J. Lankford¹⁶³, F. Lanni²⁵, K. Lantzsch³⁰, A. Lanza^{119a}, S. Laplace⁷⁸, C. Lapoire²¹, J.F. Laporte¹³⁶, T. Lari^{89a}, A. Larner¹¹⁸, M. Lassnig³⁰, P. Laurelli⁴⁷, V. Lavorini^{37a,37b}, W. Lavrijsen¹⁵, P. Laycock⁷³, O. Le Dortz⁷⁸, E. Le Guirrec⁸³, E. Le Menedeu¹², T. LeCompte⁶, F. Ledroit-Guillon⁵⁵, H. Lee¹⁰⁵, J.S.H. Lee¹¹⁶, S.C. Lee¹⁵¹, L. Lee¹⁷⁶, M. Lefebvre¹⁶⁹, M. Legendre¹³⁶, F. Legger⁹⁸, C. Leggett¹⁵, M. Lehmacher²¹, G. Lehmann Miotto³⁰, A.G. Leister¹⁷⁶, M.A.L. Leite^{24d}, R. Leitner¹²⁷, D. Lellouch¹⁷², B. Lemmer⁵⁴, V. Lendermann^{58a}, K.J.C. Leney^{145b}, T. Lenz¹⁰⁵, G. Lenzen¹⁷⁵, B. Lenzi³⁰, K. Leonhardt⁴⁴, S. Leontsinis¹⁰, F. Lepold^{58a}, C. Leroy⁹³, J.-R. Lessard¹⁶⁹, C.G. Lester²⁸, C.M. Lester¹²⁰, J. Levêque⁵, D. Levin⁸⁷, L.J. Levinson¹⁷², A. Lewis¹¹⁸, G.H. Lewis¹⁰⁸, A.M. Leyko²¹, M. Leyton¹⁶, B. Li^{33b}, B. Li⁸³, H. Li¹⁴⁸, H.L. Li³¹, S. Li^{33b,s}, X. Li⁸⁷, Z. Liang^{118,t}, H. Liao³⁴, B. Liberti^{133a}, P. Lichard³⁰, K. Lie¹⁶⁵, J. Liebal²¹, W. Liebig¹⁴, C. Limbach²¹, A. Limosani⁸⁶, M. Limper⁶², S.C. Lin^{151,u}, F. Linde¹⁰⁵, B.E. Lindquist¹⁴⁸, J.T. Linnemann⁸⁸, E. Lipeles¹²⁰, A. Lipniacka¹⁴, M. Lisovsky⁴², T.M. Liss¹⁶⁵, D. Lissauer²⁵, A. Lister¹⁶⁸, A.M. Litke¹³⁷, D. Liu¹⁵¹, J.B. Liu^{33b}, K. Liu^{33b,v}, L. Liu⁸⁷, M. Liu^{33b}, Y. Liu^{33b}, M. Livan^{119a,119b}, S.S.A. Livermore¹¹⁸, A. Lleres⁵⁵, J. Llorente Merino⁸⁰, S.L. Lloyd⁷⁵, F. Lo Sterzo^{132a,132b}, E. Lobodzinska⁴², P. Loch⁷, W.S. Lockman¹³⁷, T. Loddenkoetter²¹, F.K. Loebinger⁸², A.E. Loevschall-Jensen³⁶, A. Loginov¹⁷⁶, C.W. Loh¹⁶⁸, T. Lohse¹⁶, K. Lohwasser⁴⁸, M. Lokajicek¹²⁵, V.P. Lombardo⁵, R.E. Long⁷¹, L. Lopes^{124a}, D. Lopez Mateos⁵⁷, J. Lorenz⁹⁸,

N. Lorenzo Martinez¹¹⁵, M. Losada¹⁶², P. Loscutoff¹⁵, M.J. Losty^{159a,*}, X. Lou⁴¹, A. Lounis¹¹⁵, K.F. Loureiro¹⁶², J. Love⁶, P.A. Love⁷¹, A.J. Lowe^{143.f}, F. Lu^{33a}, H.J. Lubatti¹³⁸, C. Luci^{132a,132b}, A. Lucotte⁵⁵, D. Ludwig⁴², I. Ludwig⁴⁸, J. Ludwig⁴⁸, F. Luehring⁶⁰, W. Lukas⁶¹, L. Luminari^{132a}, E. Lund¹¹⁷, B. Lundberg⁷⁹, J. Lundberg^{146a,146b}, O. Lundberg^{146a,146b}, B. Lund-Jensen¹⁴⁷, J. Lundquist³⁶, M. Lungwitz⁸¹, D. Lynn²⁵, R. Lysak¹²⁵, E. Lytken⁷⁹, H. Ma²⁵, L.L. Ma¹⁷³, G. Maccarrone⁴⁷, A. Macchiolo⁹⁹, B. Maček⁷⁴, J. Machado Miguens^{124a}, D. Macina³⁰, R. Mackeprang³⁶, R. Madar⁴⁸, R.J. Madaras¹⁵, H.J. Maddocks⁷¹, W.F. Mader⁴⁴, A. Madsen¹⁶⁶, M. Maeno⁵, T. Maeno²⁵, L. Magnoni¹⁶³, E. Magradze⁵⁴, K. Mahboubi⁴⁸, J. Mahlstedt¹⁰⁵, S. Mahmoud⁷³, G. Mahout¹⁸, C. Maiani¹³⁶, C. Maidantchik^{24a}, A. Maio^{124a,c}, S. Majewski²⁵, Y. Makida⁶⁵, N. Makovec¹¹⁵, P. Mal^{136.w}, B. Malaescu⁷⁸, Pa. Malecki³⁹, P. Malecki³⁹, V.P. Maleev¹²¹, F. Malek⁵⁵, U. Mallik⁶², D. Malon⁶, C. Malone¹⁴³, S. Maltezos¹⁰, V. Malyshev¹⁰⁷, S. Malyukov³⁰, J. Mamuzic^{13b}, L. Mandelli^{89a}, I. Mandić⁷⁴, R. Mandrysch⁶², J. Maneira^{124a}, A. Manfredini⁹⁹, L. Manhaes de Andrade Filho^{24b}, J.A. Manjarres Ramos¹³⁶, A. Mann⁹⁸, P.M. Manning¹³⁷, A. Manousakis-Katsikakis⁹, B. Mansoulie¹³⁶, R. Mantifel⁸⁵, L. Mapelli³⁰, L. March¹⁶⁷, J.F. Marchand²⁹, F. Marchese^{133a,133b}, G. Marchiori⁷⁸, M. Marcisovsky¹²⁵, C.P. Marino¹⁶⁹, F. Marroquim^{24a}, Z. Marshall³⁰, L.F. Marti¹⁷, S. Marti-Garcia¹⁶⁷, B. Martin³⁰, B. Martin⁸⁸, J.P. Martin⁹³, T.A. Martin¹⁷⁰, V.J. Martin⁴⁶, B. Martin dit Latour⁴⁹, H. Martinez¹³⁶, M. Martinez¹², S. Martin-Haugh¹⁴⁹, A.C. Martyniuk¹⁶⁹, M. Marx⁸², F. Marzano^{132a}, A. Marzin¹¹¹, L. Masetti⁸¹, T. Mashimo¹⁵⁵, R. Mashinistov⁹⁴, J. Masik⁸², A.L. Maslennikov¹⁰⁷, I. Massa^{20a,20b}, N. Massol⁵, P. Mastrandrea¹⁴⁸, A. Mastroberardino^{37a,37b}, T. Masubuchi¹⁵⁵, H. Matsunaga¹⁵⁵, T. Matsushita⁶⁶, P. Mättig¹⁷⁵, S. Mättig⁴², C. Mattravers^{118.d}, J. Maurer⁸³, S.J. Maxfield⁷³, D.A. Maximov^{107.g}, R. Mazini¹⁵¹, M. Mazur²¹, L. Mazzaferro^{133a,133b}, M. Mazzanti^{89a}, S.P. Mc Kee⁸⁷, A. McCarn¹⁶⁵, R.L. McCarthy¹⁴⁸, T.G. McCarthy²⁹, N.A. McCubbin¹²⁹, K.W. McFarlane^{56,*}, J.A. McFayden¹³⁹, G. Mchedlidze^{51b}, T. McLaughlan¹⁸, S.J. McMahan¹²⁹, R.A. McPherson^{169.j}, A. Meade⁸⁴, J. Mechnich¹⁰⁵, M. Mechtel¹⁷⁵, M. Medinnis⁴², S. Meehan³¹, R. Meera-Lebbai¹¹¹, T. Meguro¹¹⁶, S. Mehlhase³⁶, A. Mehta⁷³, K. Meier^{58a}, C. Meineck⁹⁸, B. Meirose⁷⁹, C. Melachrinou³¹, B.R. Mellado Garcia¹⁷³, F. Meloni^{89a,89b}, L. Mendoza Navas¹⁶², A. Mengarelli^{20a,20b}, S. Menke⁹⁹, E. Meoni¹⁶¹, K.M. Mercurio⁵⁷, N. Meric¹³⁶, P. Mermoud⁴⁹, L. Merola^{102a,102b}, C. Meroni^{89a}, F.S. Merritt³¹, H. Merritt¹⁰⁹, A. Messina^{30.x}, J. Metcalfe²⁵, A.S. Mete¹⁶³, C. Meyer⁸¹, C. Meyer³¹, J-P. Meyer¹³⁶, J. Meyer³⁰, J. Meyer⁵⁴, S. Michal³⁰, R.P. Middleton¹²⁹, S. Migas⁷³, L. Mijović¹³⁶, G. Mikenberg¹⁷², M. Mikestikova¹²⁵, M. Mikuž⁷⁴, D.W. Miller³¹, R.J. Miller⁸⁸, W.J. Mills¹⁶⁸, C. Mills⁵⁷, A. Milov¹⁷², D.A. Milstead^{146a,146b}, D. Milstein¹⁷², A.A. Minaenko¹²⁸, M. Miñano Moya¹⁶⁷, I.A. Minashvili⁶⁴, A.I. Mincer¹⁰⁸, B. Mindur^{38a}, M. Mineev⁶⁴, Y. Ming¹⁷³, L.M. Mir¹², G. Mirabelli^{132a}, J. Mitrevski¹³⁷, V.A. Mitsou¹⁶⁷, S. Mitsui⁶⁵, P.S. Miyagawa¹³⁹, J.U. Mjörnmark⁷⁹, T. Moa^{146a,146b}, V. Moeller²⁸, S. Mohapatra¹⁴⁸, W. Mohr⁴⁸, R. Moles-Valls¹⁶⁷, A. Molfetas³⁰, K. Mönig⁴², C. Monini⁵⁵, J. Monk³⁶, E. Monnier⁸³, J. Montejo Berlingen¹², F. Monticelli⁷⁰, S. Monzani^{20a,20b}, R.W. Moore³, C. Mora Herrera⁴⁹, A. Moraes⁵³, N. Morange⁶², J. Morel⁵⁴, D. Moreno⁸¹, M. Moreno Llácer¹⁶⁷, P. Morettini^{50a}, M. Morgenstern⁴⁴, M. Morii⁵⁷, A.K. Morley³⁰, G. Mornacchi³⁰, J.D. Morris⁷⁵, L. Morvaj¹⁰¹, N. Möser²¹, H.G. Moser⁹⁹, M. Mosidze^{51b}, J. Moss¹⁰⁹, R. Mount¹⁴³, E. Mountricha^{10.y}, S.V. Mouraviev^{94,*}, E.J.W. Moyse⁸⁴, R.D. Mudd¹⁸, F. Mueller^{58a}, J. Mueller¹²³, K. Mueller²¹, T. Mueller²⁸, T. Mueller⁸¹, D. Muenstermann³⁰, T.A. Müller⁹⁸, Y. Munwes¹⁵³, J.A. Murillo Quijada¹⁸, W.J. Murray¹²⁹, I. Mussche¹⁰⁵, E. Musto¹⁵², A.G. Myagkov¹²⁸, M. Myska¹²⁵, O. Nackenhorst⁵⁴, J. Nadal¹², K. Nagai¹⁶⁰, R. Nagai¹⁵⁷, Y. Nagai⁸³, K. Nagano⁶⁵, A. Nagarkar¹⁰⁹, Y. Nagasaka⁵⁹, M. Nagel⁹⁹, A.M. Nairz³⁰, Y. Nakahama³⁰, K. Nakamura⁶⁵, T. Nakamura¹⁵⁵, I. Nakano¹¹⁰, H. Namasivayam⁴¹, G. Nanava²¹, A. Napier¹⁶¹, R. Narayan^{58b}, M. Nash^{77.d}, T. Nattermann²¹, T. Naumann⁴², G. Navarro¹⁶², H.A. Neal⁸⁷, P.Yu. Nechaeva⁹⁴, T.J. Neep⁸², A. Negri^{119a,119b}, G. Negri³⁰, M. Negrini^{20a}, S. Nektarijevic⁴⁹, A. Nelson¹⁶³, T.K. Nelson¹⁴³, S. Nemecek¹²⁵, P. Nemethy¹⁰⁸, A.A. Nepomuceno^{24a}, M. Nessi^{30.z}, M.S. Neubauer¹⁶⁵, M. Neumann¹⁷⁵, A. Neusiedl⁸¹, R.M. Neves¹⁰⁸, P. Nevski²⁵, F.M. Newcomer¹²⁰, P.R. Newman¹⁸, D.H. Nguyen⁶, V. Nguyen Thi Hong¹³⁶, R.B. Nickerson¹¹⁸, R. Nicolaidou¹³⁶, B. Nicquevert³⁰, F. Niedercorn¹¹⁵, J. Nielsen¹³⁷, N. Nikiforou³⁵, A. Nikiforov¹⁶, V. Nikolaenko¹²⁸, I. Nikolic-Audit⁷⁸, K. Nikolics⁴⁹, K. Nikolopoulos¹⁸, H. Nilsen⁴⁸, P. Nilsson⁸, Y. Ninomiya¹⁵⁵, A. Nisati^{132a}, R. Nisius⁹⁹, T. Nobe¹⁵⁷, L. Nodulman⁶, M. Nomachi¹¹⁶, I. Nomidis¹⁵⁴, S. Norberg¹¹¹, M. Nordberg³⁰, J. Novakova¹²⁷, M. Nozaki⁶⁵, L. Nozka¹¹³, A.-E. Nuncio-Quiroz²¹, G. Nunes Hanninger⁸⁶, T. Nunnemann⁹⁸, E. Nurse⁷⁷, B.J. O'Brien⁴⁶, D.C. O'Neil¹⁴², V. O'Shea⁵³, L.B. Oakes⁹⁸, F.G. Oakham^{29.e}, H. Oberlack⁹⁹, J. Ocariz⁷⁸, A. Ochi⁶⁶, M.I. Ochoa⁷⁷, S. Oda⁶⁹, S. Odaka⁶⁵, J. Odier⁸³, H. Ogren⁶⁰, A. Oh⁸², S.H. Oh⁴⁵, C.C. Ohm³⁰, T. Ohshima¹⁰¹, W. Okamura¹¹⁶, H. Okawa²⁵, Y. Okumura³¹, T. Okuyama¹⁵⁵, A. Olariu^{26a}, A.G. Olchevski⁶⁴, S.A. Olivares Pino⁴⁶, M. Oliveira^{124a.h}, D. Oliveira Damazio²⁵, E. Oliver Garcia¹⁶⁷, D. Olivito¹²⁰, A. Olszewski³⁹, J. Olszowska³⁹, A. Onofre^{124a.aa}, P.U.E. Onyisi^{31.ab}, C.J. Oram^{159a}, M.J. Oreglia³¹, Y. Oren¹⁵³, D. Orestano^{134a,134b}, N. Orlando^{72a,72b}, C. Oropeza Barrera⁵³, R.S. Orr¹⁵⁸, B. Osculati^{50a,50b}, R. Ospanov¹²⁰, C. Osuna¹², G. Otero y Garzon²⁷, J.P. Ottersbach¹⁰⁵, M. Ouchrif^{135d}, E.A. Ouellette¹⁶⁹, F. Ould-Saada¹¹⁷, A. Ouraou¹³⁶, Q. Ouyang^{33a}, A. Ovcharova¹⁵, M. Owen⁸², S. Owen¹³⁹, V.E. Ozcan^{19a}, N. Ozturk⁸,

A. Pacheco Pages¹², C. Padilla Aranda¹², S. Pagan Griso¹⁵, E. Paganis¹³⁹, C. Pahl⁹⁹, F. Paige²⁵, P. Pais⁸⁴, K. Pajchel¹¹⁷, G. Palacino^{159b}, C.P. Paleari⁷, S. Palestini³⁰, D. Pallin³⁴, A. Palma^{124a}, J.D. Palmer¹⁸, Y.B. Pan¹⁷³, E. Panagiotopoulou¹⁰, J.G. Panduro Vazquez⁷⁶, P. Pani¹⁰⁵, N. Panikashvili⁸⁷, S. Panitkin²⁵, D. Pantea^{26a}, A. Papadelis^{146a}, Th.D. Papadopoulos¹⁰, A. Paramonov⁶, D. Paredes Hernandez³⁴, W. Park^{25.ac}, M.A. Parker²⁸, F. Parodi^{50a,50b}, J.A. Parsons³⁵, U. Parzefall⁴⁸, S. Pashapour⁵⁴, E. Pasqualucci^{132a}, S. Passaggio^{50a}, A. Passeri^{134a}, F. Pastore^{134a,134b,*}, Fr. Pastore⁷⁶, G. Pásztor^{49.ad}, S. Patarraia¹⁷⁵, N.D. Patel¹⁵⁰, J.R. Pater⁸², S. Patricelli^{102a,102b}, T. Pauly³⁰, J. Pearce¹⁶⁹, M. Pedersen¹¹⁷, S. Pedraza Lopez¹⁶⁷, M.I. Pedraza Morales¹⁷³, S.V. Peleganchuk¹⁰⁷, D. Pelikan¹⁶⁶, H. Peng^{33b}, B. Penning³¹, A. Penson³⁵, J. Penwell⁶⁰, T. Perez Cavalcanti⁴², E. Perez Codina^{159a}, M.T. Pérez García-Estañ¹⁶⁷, V. Perez Reale³⁵, L. Perini^{89a,89b}, H. Pernegger³⁰, R. Perrino^{72a}, P. Perrodo⁵, V.D. Peshekhonov⁶⁴, K. Peters³⁰, R.F.Y. Peters^{54.ae}, B.A. Petersen³⁰, J. Petersen³⁰, T.C. Petersen³⁶, E. Petit⁵, A. Petridis^{146a,146b}, C. Petridou¹⁵⁴, E. Petrolo^{132a}, F. Petrucci^{134a,134b}, D. Petschull⁴², M. Petteni¹⁴², R. Pezoa^{32b}, A. Phan⁸⁶, P.W. Phillips¹²⁹, G. Piacquadio¹⁴³, E. Pianori¹⁷⁰, A. Picazio⁴⁹, E. Piccaro⁷⁵, M. Piccinini^{20a,20b}, S.M. Piec⁴², R. Piegaia²⁷, D.T. Pignotti¹⁰⁹, J.E. Pilcher³¹, A.D. Pilkington⁸², J. Pina^{124a.c}, M. Pinamonti^{164a,164c.af}, A. Pinder¹¹⁸, J.L. Pinfold³, A. Pingel³⁶, B. Pinto^{124a}, C. Pizio^{89a,89b}, M.-A. Pleier²⁵, V. Pleskot¹²⁷, E. Plotnikova⁶⁴, P. Plucinski^{146a,146b}, A. Poblaguev²⁵, S. Poddar^{58a}, F. Podlyski³⁴, R. Poettgen⁸¹, L. Poggioli¹¹⁵, D. Pohl²¹, M. Pohl⁴⁹, G. Polesello^{119a}, A. Policicchio^{37a,37b}, R. Polifka¹⁵⁸, A. Polini^{20a}, V. Polychronakos²⁵, D. Pomeroy²³, K. Pommès³⁰, L. Pontecorvo^{132a}, B.G. Pope⁸⁸, G.A. Popeneciu^{26a}, D.S. Popovic^{13a}, A. Poppleton³⁰, X. Portell Bueso³⁰, G.E. Pospelov⁹⁹, S. Pospisil¹²⁶, I.N. Potrap⁶⁴, C.J. Potter¹⁴⁹, C.T. Potter¹¹⁴, G. Poulard³⁰, J. Poveda⁶⁰, V. Pozdnyakov⁶⁴, R. Prabhu⁷⁷, P. Pralavorio⁸³, A. Pranko¹⁵, S. Prasad³⁰, R. Pravahan²⁵, S. Prell⁶³, K. Pretzl¹⁷, D. Price⁶⁰, J. Price⁷³, L.E. Price⁶, D. Prieur¹²³, M. Primavera^{72a}, M. Proissl⁴⁶, K. Prokofiev¹⁰⁸, F. Prokoshin^{32b}, E. Protopapadaki¹³⁶, S. Protopopescu²⁵, J. Proudfoot⁶, X. Prudent⁴⁴, M. Przybycien^{38a}, H. Przysiezniak⁵, S. Psoroulas²¹, E. Ptacek¹¹⁴, E. Pueschel⁸⁴, D. Pulton¹⁴⁸, M. Purohit^{25.ac}, P. Puzo¹¹⁵, Y. Pylypchenko⁶², J. Qian⁸⁷, A. Quadt⁵⁴, D.R. Quarrie¹⁵, W.B. Quayle¹⁷³, D. Quilty⁵³, M. Raas¹⁰⁴, V. Radeka²⁵, V. Radescu⁴², P. Radloff¹¹⁴, F. Ragusa^{89a,89b}, G. Rahal¹⁷⁸, S. Rajagopalan²⁵, M. Rammensee⁴⁸, M. Rammes¹⁴¹, A.S. Randle-Conde⁴⁰, K. Randrianarivony²⁹, C. Rangel-Smith⁷⁸, K. Rao¹⁶³, F. Rauscher⁹⁸, T.C. Rave⁴⁸, T. Ravenscroft⁵³, M. Raymond³⁰, A.L. Read¹¹⁷, D.M. Rebuffi^{119a,119b}, A. Redelbach¹⁷⁴, G. Redlinger²⁵, R. Reece¹²⁰, K. Reeves⁴¹, A. Reinsch¹¹⁴, I. Reisinger⁴³, M. Relich¹⁶³, C. Rembser³⁰, Z.L. Ren¹⁵¹, A. Renaud¹¹⁵, M. Rescigno^{132a}, S. Resconi^{89a}, B. Resende¹³⁶, P. Reznicek⁹⁸, R. Rezvani⁵⁸, L. Richter⁹⁹, E. Richter-Was^{38b}, M. Ridel⁷⁸, P. Rieck¹⁶, M. Rijssenbeek¹⁴⁸, A. Rimoldi^{119a,119b}, L. Rinaldi^{20a}, R.R. Rios⁴⁰, E. Ritsch⁶¹, I. Riu¹², G. Rivoltella^{89a,89b}, F. Rizatdinova¹¹², E. Rizvi⁷⁵, S.H. Robertson^{85.j}, A. Robichaud-Veronneau¹¹⁸, D. Robinson²⁸, J.E.M. Robinson⁸², A. Robson⁵³, J.G. Rocha de Lima¹⁰⁶, C. Roda^{122a,122b}, D. Roda Dos Santos³⁰, A. Roe⁵⁴, S. Roe³⁰, O. Røhne¹¹⁷, S. Rolli¹⁶¹, A. Romaniouk⁹⁶, M. Romano^{20a,20b}, G. Romeo²⁷, E. Romero Adam¹⁶⁷, N. Rompotis¹³⁸, L. Roos⁷⁸, E. Ros¹⁶⁷, S. Rosati^{132a}, K. Rosbach⁴⁹, A. Rose¹⁴⁹, M. Rose⁷⁶, G.A. Rosenbaum¹⁵⁸, P.L. Rosendahl¹⁴, O. Rosenthal¹⁴¹, L. Rossetlet⁴⁹, V. Rossetti¹², E. Rossi^{132a,132b}, L.P. Rossi^{50a}, M. Rotaru^{26a}, I. Roth¹⁷², J. Rothberg¹³⁸, D. Rousseau¹¹⁵, C.R. Royon¹³⁶, A. Rozanov⁸³, Y. Rozen¹⁵², X. Ruan^{33a.ag}, F. Rubbo¹², I. Rubinskiy⁴², N. Ruckstuhl¹⁰⁵, V.I. Rud⁹⁷, C. Rudolph⁴⁴, M.S. Rudolph¹⁵⁸, F. Rühr⁷, A. Ruiz-Martinez⁶³, L. Rummyantsev⁶⁴, Z. Rurikova⁴⁸, N.A. Rusakovich⁶⁴, A. Ruschke⁹⁸, J.P. Rutherford⁷, N. Ruthmann⁴⁸, P. Ruzicka¹²⁵, Y.F. Ryabov¹²¹, M. Rybar¹²⁷, G. Rybkin¹¹⁵, N.C. Ryder¹¹⁸, A.F. Saavedra¹⁵⁰, A. Saddique³, I. Sadeh¹⁵³, H.F.W. Sadrozinski¹³⁷, R. Sadykov⁶⁴, F. Safai Tehrani^{132a}, H. Sakamoto¹⁵⁵, G. Salamanna⁷⁵, A. Salamon^{133a}, M. Saleem¹¹¹, D. Salek³⁰, D. Salihagic⁹⁹, A. Salnikov¹⁴³, J. Salt¹⁶⁷, B.M. Salvachua Ferrando⁶, D. Salvatore^{37a,37b}, F. Salvatore¹⁴⁹, A. Salvucci¹⁰⁴, A. Salzburger³⁰, D. Sampsonidis¹⁵⁴, A. Sanchez^{102a,102b}, J. Sánchez¹⁶⁷, V. Sanchez Martinez¹⁶⁷, H. Sandaker¹⁴, H.G. Sander⁸¹, M.P. Sanders⁹⁸, M. Sandhoff¹⁷⁵, T. Sandoval²⁸, C. Sandoval¹⁶², R. Sandstroem⁹⁹, D.P.C. Sankey¹²⁹, A. Sansoni⁴⁷, C. Santoni³⁴, R. Santonico^{133a,133b}, H. Santos^{124a}, I. Santoyo Castillo¹⁴⁹, K. Sapp¹²³, J.G. Saraiva^{124a}, T. Sarangi¹⁷³, E. Sarkisyan-Grinbaum⁸, B. Sarrazin²¹, F. Sarri^{122a,122b}, G. Sartiso¹⁷⁵, O. Sasaki⁶⁵, Y. Sasaki¹⁵⁵, N. Sasao⁶⁷, I. Satsounkevitch⁹⁰, G. Sauvage^{5.*}, E. Sauvan⁵, J.B. Sauvan¹¹⁵, P. Savard^{158.e}, V. Savinov¹²³, D.O. Savu³⁰, C. Sawyer¹¹⁸, L. Sawyer^{25.l}, D.H. Saxon⁵³, J. Saxon¹²⁰, C. Sbarra^{20a}, A. Sbrizzi³, D.A. Scannicchio¹⁶³, M. Scarcella¹⁵⁰, J. Schaarschmidt¹¹⁵, P. Schacht⁹⁹, D. Schaefer¹²⁰, A. Schaelicke⁴⁶, S. Schaepe²¹, S. Schaetzel^{58b}, U. Schäfer⁸¹, A.C. Schaffer¹¹⁵, D. Schaile⁹⁸, R.D. Schamberger¹⁴⁸, V. Scharf^{58a}, V.A. Schegelsky¹²¹, D. Scheirich⁸⁷, M. Schernau¹⁶³, M.I. Scherzer³⁵, C. Schiavi^{50a,50b}, J. Schieck⁹⁸, C. Schillo⁴⁸, M. Schioppa^{37a,37b}, S. Schlenker³⁰, E. Schmidt⁴⁸, K. Schmieden²¹, C. Schmitt⁸¹, C. Schmitt⁹⁸, S. Schmitt^{58b}, B. Schneider¹⁷, Y.J. Schnellbach⁷³, U. Schnoor⁴⁴, L. Schoeffel¹³⁶, A. Schoening^{58b}, A.L.S. Schorlemmer⁵⁴, M. Schott⁸¹, D. Schouten^{159a}, J. Schovancova¹²⁵, M. Schram⁸⁵, C. Schroeder⁸¹, N. Schroer^{58c}, M.J. Schultens²¹, J. Schultes¹⁷⁵, H.-C. Schultz-Coulon^{58a}, H. Schulz¹⁶, M. Schumacher⁴⁸, B.A. Schumm¹³⁷, Ph. Schune¹³⁶, A. Schwartzman¹⁴³, Ph. Schwegler⁹⁹, Ph. Schwemling¹³⁶, R. Schwienhorst⁸⁸, J. Schwindling¹³⁶, T. Schwindt²¹, M. Schwoerer⁵, F.G. Sciaccia¹⁷, E. Scifo¹¹⁵, G. Sciolla²³, W.G. Scott¹²⁹, F. Scutti²¹, J. Searcy⁸⁷, G. Sedov⁴²,

E. Sedykh¹²¹, S.C. Seidel¹⁰³, A. Seiden¹³⁷, F. Seifert⁴⁴, J.M. Seixas^{24a}, G. Sekhniaidze^{102a}, S.J. Sekula⁴⁰,
 K.E. Selbach⁴⁶, D.M. Seliverstov¹²¹, G. Sellers⁷³, M. Seman^{144b}, N. Semprini-Cesari^{20a,20b}, C. Serfon³⁰,
 L. Serin¹¹⁵, L. Serkin⁵⁴, T. Serre⁸³, R. Seuster^{159a}, H. Severini¹¹¹, A. Sfyrta³⁰, E. Shabalina⁵⁴, M. Shamim¹¹⁴,
 L.Y. Shan^{33a}, J.T. Shank²², Q.T. Shao⁸⁶, M. Shapiro¹⁵, P.B. Shatalov⁹⁵, K. Shaw^{164a,164c}, P. Sherwood⁷⁷,
 S. Shimizu¹⁰¹, M. Shimojima¹⁰⁰, T. Shin⁵⁶, M. Shiyakova⁶⁴, A. Shmeleva⁹⁴, M.J. Shochet³¹, D. Short¹¹⁸,
 S. Shrestha⁶³, E. Shulga⁹⁶, M.A. Shupe⁷, P. Sicho¹²⁵, A. Sidoti^{132a}, F. Siegert⁴⁸, Dj. Sijacki^{13a}, O. Silbert¹⁷²,
 J. Silva^{124a}, Y. Silver¹⁵³, D. Silverstein¹⁴³, S.B. Silverstein^{146a}, V. Simak¹²⁶, O. Simard⁵, Lj. Simic^{13a},
 S. Simion¹¹⁵, E. Simioni⁸¹, B. Simmons⁷⁷, R. Simoniello^{89a,89b}, M. Simonyan³⁶, P. Sinervo¹⁵⁸, N.B. Sinev¹¹⁴,
 V. Sipica¹⁴¹, G. Siragusa¹⁷⁴, A. Sircar²⁵, A.N. Sisakyan^{64,*}, S.Yu. Sivoklokov⁹⁷, J. Sjölin^{146a,146b}, T.B. Sjursen¹⁴,
 L.A. Skinnari¹⁵, H.P. Skottowe⁵⁷, K. Skovpen¹⁰⁷, P. Skubic¹¹¹, M. Slater¹⁸, T. Slavicek¹²⁶, K. Sliwa¹⁶¹,
 V. Smakhtin¹⁷², B.H. Smart⁴⁶, L. Smestad¹¹⁷, S.Yu. Smirnov⁹⁶, Y. Smirnov⁹⁶, L.N. Smirnova^{97,ah},
 O. Smirnova⁷⁹, K.M. Smith⁵³, M. Smizanska⁷¹, K. Smolek¹²⁶, A.A. Snesarev⁹⁴, G. Snidero⁷⁵, J. Snow¹¹¹,
 S. Snyder²⁵, R. Sobie^{169,j}, J. Sodomka¹²⁶, A. Soffer¹⁵³, D.A. Soh^{151,i}, C.A. Solans³⁰, M. Solar¹²⁶, J. Solc¹²⁶,
 E.Yu. Soldatov⁹⁶, U. Soldevila¹⁶⁷, E. Solfaroli Camillocci^{132a,132b}, A.A. Solodkov¹²⁸, O.V. Solovyanov¹²⁸,
 V. Solovyev¹²¹, N. Soni¹, A. Sood¹⁵, V. Sopko¹²⁶, B. Sopko¹²⁶, M. Sosebee⁸, R. Soualah^{164a,164c}, P. Soueid⁹³,
 A. Soukharev¹⁰⁷, D. South⁴², S. Spagnolo^{72a,72b}, F. Spanò⁷⁶, R. Spighi^{20a}, G. Spigo³⁰, R. Spiwoks³⁰,
 M. Spousta^{127,ai}, T. Spreitzer¹⁵⁸, B. Spurlock⁸, R.D. St. Denis⁵³, J. Stahlman¹²⁰, R. Stamen^{58a}, E. Stanecka³⁹,
 R.W. Stanek⁶, C. Stanescu^{134a}, M. Stanescu-Bellu⁴², M.M. Stanitzki⁴², S. Stapnes¹¹⁷, E.A. Starchenko¹²⁸,
 J. Stark⁵⁵, P. Staroba¹²⁵, P. Starovoitov⁴², R. Staszewski³⁹, A. Staude⁹⁸, P. Stavina^{144a,*}, G. Steele⁵³,
 P. Steinbach⁴⁴, P. Steinberg²⁵, I. Stekl¹²⁶, B. Stelzer¹⁴², H.J. Stelzer⁸⁸, O. Stelzer-Chilton^{159a}, H. Stenzel⁵²,
 S. Stern⁹⁹, G.A. Stewart³⁰, J.A. Stillings²¹, M.C. Stockton⁸⁵, M. Stoebe⁸⁵, K. Stoerig⁴⁸, G. Stoicea^{26a},
 S. Stonjek⁹⁹, A.R. Stradling⁸, A. Straessner⁴⁴, J. Strandberg¹⁴⁷, S. Strandberg^{146a,146b}, A. Strandlie¹¹⁷,
 M. Strang¹⁰⁹, E. Strauss¹⁴³, M. Strauss¹¹¹, P. Strizenec^{144b}, R. Ströhmer¹⁷⁴, D.M. Strom¹¹⁴, J.A. Strong^{76,*},
 R. Stroynowski⁴⁰, B. Stugu¹⁴, I. Stumer^{25,*}, J. Stupak¹⁴⁸, P. Sturm¹⁷⁵, N.A. Styles⁴², D. Su¹⁴³, H.S. Subramania³,
 R. Subramaniam²⁵, A. Succurro¹², Y. Sugaya¹¹⁶, C. Suhr¹⁰⁶, M. Suk¹²⁶, V.V. Sulin⁹⁴, S. Sultansoy^{4c},
 T. Sumida⁶⁷, X. Sun⁵⁵, J.E. Sundermann⁴⁸, K. Suruliz¹³⁹, G. Susinno^{37a,37b}, M.R. Sutton¹⁴⁹, Y. Suzuki⁶⁵,
 Y. Suzuki⁶⁶, M. Svatos¹²⁵, S. Swedish¹⁶⁸, M. Swiatlowski¹⁴³, I. Sykora^{144a}, T. Sykora¹²⁷, D. Ta¹⁰⁵,
 K. Tackmann⁴², A. Taffard¹⁶³, R. Tafirout^{159a}, N. Taiblum¹⁵³, Y. Takahashi¹⁰¹, H. Takai²⁵, R. Takashima⁶⁸,
 H. Takeda⁶⁶, T. Takeshita¹⁴⁰, Y. Takubo⁶⁵, M. Talby⁸³, A. Talyshev^{107,g}, J.Y.C. Tam¹⁷⁴, M.C. Tamsett²⁵,
 K.G. Tan⁸⁶, J. Tanaka¹⁵⁵, R. Tanaka¹¹⁵, S. Tanaka¹³¹, S. Tanaka⁶⁵, A.J. Tanasijczuk¹⁴², K. Tani⁶⁶, N. Tannoury⁸³,
 S. Tapprogge⁸¹, D. Tardif¹⁵⁸, S. Tarem¹⁵², F. Tarrade²⁹, G.F. Tartarelli^{89a}, P. Tas¹²⁷, M. Tasevsky¹²⁵,
 E. Tassi^{37a,37b}, Y. Tayalati^{135d}, C. Taylor⁷⁷, F.E. Taylor⁹², G.N. Taylor⁸⁶, W. Taylor^{159b}, M. Teinturier¹¹⁵,
 F.A. Teischinger³⁰, M. Teixeira Dias Castanheira⁷⁵, P. Teixeira-Dias⁷⁶, K.K. Temming⁴⁸, H. Ten Kate³⁰,
 P.K. Teng¹⁵¹, S. Terada⁶⁵, K. Terashi¹⁵⁵, J. Terron⁸⁰, M. Testa⁴⁷, R.J. Teuscher^{158,j}, J. Therhaag²¹,
 T. Theveneaux-Pelzer³⁴, S. Thoma⁴⁸, J.P. Thomas¹⁸, E.N. Thompson³⁵, P.D. Thompson¹⁸, P.D. Thompson¹⁵⁸,
 A.S. Thompson⁵³, L.A. Thomsen³⁶, E. Thomson¹²⁰, M. Thomson²⁸, W.M. Thong⁸⁶, R.P. Thun^{87,*}, F. Tian³⁵,
 M.J. Tibbetts¹⁵, T. Tic¹²⁵, V.O. Tikhomirov⁹⁴, Y.A. Tikhonov^{107,g}, S. Timoshenko⁹⁶, E. Tiouchichine⁸³,
 P. Tipton¹⁷⁶, S. Tisserant⁸³, T. Todorov⁵, S. Todorova-Nova¹⁶¹, B. Toggerson¹⁶³, J. Tojo⁶⁹, S. Tokár^{144a},
 K. Tokushuku⁶⁵, K. Tollefson⁸⁸, L. Tomlinson⁸², M. Tomoto¹⁰¹, L. Tompkins³¹, K. Toms¹⁰³, A. Tonoyan¹⁴,
 C. Topfel¹⁷, N.D. Topilin⁶⁴, E. Torrence¹¹⁴, H. Torres⁷⁸, E. Torró Pastor¹⁶⁷, J. Toth^{83,ad}, F. Touchard⁸³,
 D.R. Tovey¹³⁹, H.L. Tran¹¹⁵, T. Trefzger¹⁷⁴, L. Tremblet³⁰, A. Tricoli³⁰, I.M. Trigger^{159a}, S. Trincz-Duvoid⁷⁸,
 M.F. Tripana⁷⁰, N. Triplett²⁵, W. Trischuk¹⁵⁸, B. Trocmé⁵⁵, C. Troncon^{89a}, M. Trottier-McDonald¹⁴²,
 M. Trovatelli^{134a,134b}, P. True⁸⁸, M. Trzebinski³⁹, A. Trzupek³⁹, C. Tsarouchas³⁰, J.C-L. Tseng¹¹⁸,
 M. Tsiakiris¹⁰⁵, P.V. Tsiarehka⁹⁰, D. Tsionou¹³⁶, G. Tsiopolitis¹⁰, S. Tsiskaridze¹², V. Tsiskaridze⁴⁸,
 E.G. Tskhadadze^{51a}, I.I. Tsukerman⁹⁵, V. Tsulaia¹⁵, J.-W. Tsung²¹, S. Tsuno⁶⁵, D. Tsybychev¹⁴⁸, A. Tua¹³⁹,
 A. Tudorache^{26a}, V. Tudorache^{26a}, J.M. Tuggle³¹, A.N. Tuna¹²⁰, M. Turala³⁹, D. Turecek¹²⁶, I. Turk Cakir^{4d},
 R. Turra^{89a,89b}, P.M. Tuts³⁵, A. Tykhonov⁷⁴, M. Tylmad^{146a,146b}, M. Tyndel¹²⁹, G. Tzanakos⁹, K. Uchida²¹,
 I. Ueda¹⁵⁵, R. Ueno²⁹, M. Ughetto⁸³, M. Uglan¹⁴, M. Uhlenbrock²¹, F. Ukegawa¹⁶⁰, G. Unal³⁰, A. Undrus²⁵,
 G. Unel¹⁶³, F.C. Ungaro⁴⁸, Y. Unno⁶⁵, D. Urbaniec³⁵, P. Urquijo²¹, G. Usai⁸, L. Vacavant⁸³, V. Vacek¹²⁶,
 B. Vachon⁸⁵, S. Vahsen¹⁵, N. Valencic¹⁰⁵, S. Valentineti^{20a,20b}, A. Valero¹⁶⁷, L. Valery³⁴, S. Valkar¹²⁷,
 E. Valladolid Gallego¹⁶⁷, S. Vallecorsa¹⁵², J.A. Valls Ferrer¹⁶⁷, R. Van Berg¹²⁰, P.C. Van Der Deijl¹⁰⁵,
 R. van der Geer¹⁰⁵, H. van der Graaf¹⁰⁵, R. Van Der Leeuw¹⁰⁵, E. van der Poel¹⁰⁵, D. van der Ster³⁰,
 N. van Eldik³⁰, P. van Gemmeren⁶, J. Van Nieuwkoop¹⁴², I. van Vulpen¹⁰⁵, M. Vanadia⁹⁹, W. Vandelli³⁰,
 A. Vaniachine⁶, P. Vankov⁴², F. Vannucci⁷⁸, R. Vari^{132a}, E.W. Varnes⁷, T. Varol⁸⁴, D. Varouchas¹⁵,
 A. Vartapetian⁸, K.E. Varvell¹⁵⁰, V.I. Vassilakopoulos⁵⁶, F. Vazeille³⁴, T. Vazquez Schroeder⁵⁴, F. Veloso^{124a},
 S. Veneziano^{132a}, A. Ventura^{72a,72b}, D. Ventura⁸⁴, M. Venturi⁴⁸, N. Venturi¹⁵⁸, V. Vercesi^{119a}, M. Verducci¹³⁸,
 W. Verkerke¹⁰⁵, J.C. Vermeulen¹⁰⁵, A. Vest⁴⁴, M.C. Vetterli^{142,e}, I. Vichou¹⁶⁵, T. Vickey^{145b,aj},

O.E. Vickey Boeriu^{145b}, G.H.A. Viehhauser¹¹⁸, S. Viel¹⁶⁸, M. Villa^{20a,20b}, M. Villaplana Perez¹⁶⁷, E. Vilucchi⁴⁷, M.G. Vinciter²⁹, V.B. Vinogradov⁶⁴, J. Virzi¹⁵, O. Vitells¹⁷², M. Viti⁴², I. Vivarelli⁴⁸, F. Vives Vaque³, S. Vlachos¹⁰, D. Vladiou⁹⁸, M. Vlasak¹²⁶, A. Vogel²¹, P. Vokac¹²⁶, G. Volpi⁴⁷, M. Volpi⁸⁶, G. Volpini^{89a}, H. von der Schmitt⁹⁹, H. von Radziewski⁴⁸, E. von Toerne²¹, V. Vorobel¹²⁷, M. Vos¹⁶⁷, R. Voss³⁰, J.H. Vossebeld⁷³, N. Vranjes¹³⁶, M. Vranjes Milosavljevic¹⁰⁵, V. Vrba¹²⁵, M. Vreeswijk¹⁰⁵, T. Vu Anh⁴⁸, R. Vuillermet³⁰, I. Vukotic³¹, Z. Vykydal¹²⁶, W. Wagner¹⁷⁵, P. Wagner²¹, H. Wahlen¹⁷⁵, S. Wahrenmund⁴⁴, J. Wakabayashi¹⁰¹, S. Walch⁸⁷, J. Walder⁷¹, R. Walker⁹⁸, W. Walkowiak¹⁴¹, R. Wall¹⁷⁶, P. Waller⁷³, B. Walsh¹⁷⁶, C. Wang⁴⁵, H. Wang¹⁷³, H. Wang⁴⁰, J. Wang¹⁵¹, J. Wang^{33a}, K. Wang⁸⁵, R. Wang¹⁰³, S.M. Wang¹⁵¹, T. Wang²¹, X. Wang¹⁷⁶, A. Warburton⁸⁵, C.P. Ward²⁸, D.R. Wardrope⁷⁷, M. Warsinsky⁴⁸, A. Washbrook⁴⁶, C. Wasicki⁴², I. Watanabe⁶⁶, P.M. Watkins¹⁸, A.T. Watson¹⁸, I.J. Watson¹⁵⁰, M.F. Watson¹⁸, G. Watts¹³⁸, S. Watts⁸², A.T. Waugh¹⁵⁰, B.M. Waugh⁷⁷, M.S. Weber¹⁷, J.S. Webster³¹, A.R. Weidberg¹¹⁸, P. Weigell⁹⁹, J. Weingarten⁵⁴, C. Weiser⁴⁸, P.S. Wells³⁰, T. Wenaus²⁵, D. Wendland¹⁶, Z. Weng^{151,t}, T. Wengler³⁰, S. Wenig³⁰, N. Vermes²¹, M. Werner⁴⁸, P. Werner³⁰, M. Werth¹⁶³, M. Wessels^{58a}, J. Wetter¹⁶¹, K. Whalen²⁹, A. White⁸, M.J. White⁸⁶, S. White^{122a,122b}, S.R. Whitehead¹¹⁸, D. Whiteson¹⁶³, D. Whittington⁶⁰, D. Wicke¹⁷⁵, F.J. Wickens¹²⁹, W. Wiedenmann¹⁷³, M. Wielers⁷⁹, P. Wienemann²¹, C. Wiglesworth³⁶, L.A.M. Wiik-Fuchs²¹, P.A. Wijeratne⁷⁷, A. Wildauer⁹⁹, M.A. Wildt^{42,q}, I. Wilhelm¹²⁷, H.G. Wilkens³⁰, J.Z. Will⁹⁸, E. Williams³⁵, H.H. Williams¹²⁰, S. Williams²⁸, W. Willis^{35,*}, S. Willocq⁸⁴, J.A. Wilson¹⁸, A. Wilson⁸⁷, I. Wingerter-Seez⁵, S. Winkelmann⁴⁸, F. Winklmeier³⁰, M. Wittgen¹⁴³, T. Wittig⁴³, J. Wittkowski⁹⁸, S.J. Wollstadt⁸¹, M.W. Wolter³⁹, H. Wolters^{124a,h}, W.C. Wong⁴¹, G. Wooden⁸⁷, B.K. Wosiek³⁹, J. Wotschack³⁰, M.J. Woudstra⁸², K.W. Wozniak³⁹, K. Wraight⁵³, M. Wright⁵³, B. Wrona⁷³, S.L. Wu¹⁷³, X. Wu⁴⁹, Y. Wu⁸⁷, E. Wulf³⁵, B.M. Wynne⁴⁶, S. Xella³⁶, M. Xiao¹³⁶, S. Xie⁴⁸, C. Xu^{33b,y}, D. Xu^{33a}, L. Xu^{33b}, B. Yabsley¹⁵⁰, S. Yacoub^{145a,ak}, M. Yamada⁶⁵, H. Yamaguchi¹⁵⁵, Y. Yamaguchi¹⁵⁵, A. Yamamoto⁶⁵, K. Yamamoto⁶³, S. Yamamoto¹⁵⁵, T. Yamamura¹⁵⁵, T. Yamanaka¹⁵⁵, K. Yamauchi¹⁰¹, T. Yamazaki¹⁵⁵, Y. Yamazaki⁶⁶, Z. Yan²², H. Yang^{33e}, H. Yang¹⁷³, U.K. Yang⁸², Y. Yang¹⁰⁹, Z. Yang^{146a,146b}, S. Yanush⁹¹, L. Yao^{33a}, Y. Yasu⁶⁵, E. Yatsenko⁴², K.H. Yau Wong²¹, J. Ye⁴⁰, S. Ye²⁵, A.L. Yen⁵⁷, E. Yildirim⁴², M. Yilmaz^{4b}, R. Yoosofmiya¹²³, K. Yorita¹⁷¹, R. Yoshida⁶, K. Yoshihara¹⁵⁵, C. Young¹⁴³, C.J.S. Young¹¹⁸, S. Youssef²², D. Yu²⁵, D.R. Yu¹⁵, J. Yu⁸, J. Yu¹¹², L. Yuan⁶⁶, A. Yurkewicz¹⁰⁶, B. Zabinski³⁹, R. Zaidan⁶², A.M. Zaitsev¹²⁸, S. Zambito²³, L. Zanello^{132a,132b}, D. Zanzi⁹⁹, A. Zaytsev²⁵, C. Zeitnitz¹⁷⁵, M. Zeman¹²⁶, A. Zemla³⁹, O. Zenin¹²⁸, T. Zenis^{144a}, D. Zerwas¹¹⁵, G. Zevi della Porta⁵⁷, D. Zhang⁸⁷, H. Zhang⁸⁸, J. Zhang⁶, L. Zhang¹⁵¹, X. Zhang^{33d}, Z. Zhang¹¹⁵, Z. Zhao^{33b}, A. Zhemchugov⁶⁴, J. Zhong¹¹⁸, B. Zhou⁸⁷, N. Zhou¹⁶³, Y. Zhou¹⁵¹, C.G. Zhu^{33d}, H. Zhu⁴², J. Zhu⁸⁷, Y. Zhu^{33b}, X. Zhuang^{33a}, V. Zhuravlov⁹⁹, A. Zibell⁹⁸, D. Zieminska⁶⁰, N.I. Zimin⁶⁴, R. Zimmermann²¹, S. Zimmermann²¹, S. Zimmermann⁴⁸, Z. Zinonos^{122a,122b}, M. Ziolkowski¹⁴¹, R. Zitoun⁵, L. Živković³⁵, V.V. Zmouchko^{128,*}, G. Zobernig¹⁷³, A. Zoccoli^{20a,20b}, M. zur Nedden¹⁶, V. Zutshi¹⁰⁶, L. Zwalinski³⁰.

¹ School of Chemistry and Physics, University of Adelaide, Adelaide, Australia

² Physics Department, SUNY Albany, Albany NY, United States of America

³ Department of Physics, University of Alberta, Edmonton AB, Canada

⁴ (a) Department of Physics, Ankara University, Ankara; (b) Department of Physics, Gazi University, Ankara; (c) Division of Physics, TOBB University of Economics and Technology, Ankara; (d) Turkish Atomic Energy Authority, Ankara, Turkey

⁵ LAPP, CNRS/IN2P3 and Université de Savoie, Annecy-le-Vieux, France

⁶ High Energy Physics Division, Argonne National Laboratory, Argonne IL, United States of America

⁷ Department of Physics, University of Arizona, Tucson AZ, United States of America

⁸ Department of Physics, The University of Texas at Arlington, Arlington TX, United States of America

⁹ Physics Department, University of Athens, Athens, Greece

¹⁰ Physics Department, National Technical University of Athens, Zografou, Greece

¹¹ Institute of Physics, Azerbaijan Academy of Sciences, Baku, Azerbaijan

¹² Institut de Física d'Altes Energies and Departament de Física de la Universitat Autònoma de Barcelona and ICREA, Barcelona, Spain

¹³ (a) Institute of Physics, University of Belgrade, Belgrade; (b) Vinca Institute of Nuclear Sciences, University of Belgrade, Belgrade, Serbia

¹⁴ Department for Physics and Technology, University of Bergen, Bergen, Norway

¹⁵ Physics Division, Lawrence Berkeley National Laboratory and University of California, Berkeley CA, United States of America

¹⁶ Department of Physics, Humboldt University, Berlin, Germany

¹⁷ Albert Einstein Center for Fundamental Physics and Laboratory for High Energy Physics, University of Bern, Bern, Switzerland

- 18 School of Physics and Astronomy, University of Birmingham, Birmingham, United Kingdom
- 19 (a) Department of Physics, Bogazici University, Istanbul; (b) Division of Physics, Dogus University, Istanbul; (c) Department of Physics Engineering, Gaziantep University, Gaziantep, Turkey
- 20 (a) INFN Sezione di Bologna; (b) Dipartimento di Fisica, Università di Bologna, Bologna, Italy
- 21 Physikalisches Institut, University of Bonn, Bonn, Germany
- 22 Department of Physics, Boston University, Boston MA, United States of America
- 23 Department of Physics, Brandeis University, Waltham MA, United States of America
- 24 (a) Universidade Federal do Rio De Janeiro COPPE/EE/IF, Rio de Janeiro; (b) Federal University of Juiz de Fora (UFJF), Juiz de Fora; (c) Federal University of Sao Joao del Rei (UFSJ), Sao Joao del Rei; (d) Instituto de Fisica, Universidade de Sao Paulo, Sao Paulo, Brazil
- 25 Physics Department, Brookhaven National Laboratory, Upton NY, United States of America
- 26 (a) National Institute of Physics and Nuclear Engineering, Bucharest; (b) University Politehnica Bucharest, Bucharest; (c) West University in Timisoara, Timisoara, Romania
- 27 Departamento de Física, Universidad de Buenos Aires, Buenos Aires, Argentina
- 28 Cavendish Laboratory, University of Cambridge, Cambridge, United Kingdom
- 29 Department of Physics, Carleton University, Ottawa ON, Canada
- 30 CERN, Geneva, Switzerland
- 31 Enrico Fermi Institute, University of Chicago, Chicago IL, United States of America
- 32 (a) Departamento de Física, Pontificia Universidad Católica de Chile, Santiago; (b) Departamento de Física, Universidad Técnica Federico Santa María, Valparaíso, Chile
- 33 (a) Institute of High Energy Physics, Chinese Academy of Sciences, Beijing; (b) Department of Modern Physics, University of Science and Technology of China, Anhui; (c) Department of Physics, Nanjing University, Jiangsu; (d) School of Physics, Shandong University, Shandong; (e) Physics Department, Shanghai Jiao Tong University, Shanghai, China
- 34 Laboratoire de Physique Corpusculaire, Clermont Université and Université Blaise Pascal and CNRS/IN2P3, Clermont-Ferrand, France
- 35 Nevis Laboratory, Columbia University, Irvington NY, United States of America
- 36 Niels Bohr Institute, University of Copenhagen, Kobenhavn, Denmark
- 37 (a) INFN Gruppo Collegato di Cosenza; (b) Dipartimento di Fisica, Università della Calabria, Rende, Italy
- 38 (a) AGH University of Science and Technology, Faculty of Physics and Applied Computer Science, Krakow; (b) Marian Smoluchowski Institute of Physics, Jagiellonian University, Krakow, Poland
- 39 The Henryk Niewodniczanski Institute of Nuclear Physics, Polish Academy of Sciences, Krakow, Poland
- 40 Physics Department, Southern Methodist University, Dallas TX, United States of America
- 41 Physics Department, University of Texas at Dallas, Richardson TX, United States of America
- 42 DESY, Hamburg and Zeuthen, Germany
- 43 Institut für Experimentelle Physik IV, Technische Universität Dortmund, Dortmund, Germany
- 44 Institut für Kern- und Teilchenphysik, Technical University Dresden, Dresden, Germany
- 45 Department of Physics, Duke University, Durham NC, United States of America
- 46 SUPA - School of Physics and Astronomy, University of Edinburgh, Edinburgh, United Kingdom
- 47 INFN Laboratori Nazionali di Frascati, Frascati, Italy
- 48 Fakultät für Mathematik und Physik, Albert-Ludwigs-Universität, Freiburg, Germany
- 49 Section de Physique, Université de Genève, Geneva, Switzerland
- 50 (a) INFN Sezione di Genova; (b) Dipartimento di Fisica, Università di Genova, Genova, Italy
- 51 (a) E. Andronikashvili Institute of Physics, Iv. Javakishvili Tbilisi State University, Tbilisi; (b) High Energy Physics Institute, Tbilisi State University, Tbilisi, Georgia
- 52 II Physikalisches Institut, Justus-Liebig-Universität Giessen, Giessen, Germany
- 53 SUPA - School of Physics and Astronomy, University of Glasgow, Glasgow, United Kingdom
- 54 II Physikalisches Institut, Georg-August-Universität, Göttingen, Germany
- 55 Laboratoire de Physique Subatomique et de Cosmologie, Université Joseph Fourier and CNRS/IN2P3 and Institut National Polytechnique de Grenoble, Grenoble, France
- 56 Department of Physics, Hampton University, Hampton VA, United States of America
- 57 Laboratory for Particle Physics and Cosmology, Harvard University, Cambridge MA, United States of America
- 58 (a) Kirchhoff-Institut für Physik, Ruprecht-Karls-Universität Heidelberg, Heidelberg; (b) Physikalisches Institut, Ruprecht-Karls-Universität Heidelberg, Heidelberg; (c) ZITI Institut für technische Informatik, Ruprecht-Karls-Universität Heidelberg, Mannheim, Germany
- 59 Faculty of Applied Information Science, Hiroshima Institute of Technology, Hiroshima, Japan
- 60 Department of Physics, Indiana University, Bloomington IN, United States of America

- ⁶¹ Institut für Astro- und Teilchenphysik, Leopold-Franzens-Universität, Innsbruck, Austria
- ⁶² University of Iowa, Iowa City IA, United States of America
- ⁶³ Department of Physics and Astronomy, Iowa State University, Ames IA, United States of America
- ⁶⁴ Joint Institute for Nuclear Research, JINR Dubna, Dubna, Russia
- ⁶⁵ KEK, High Energy Accelerator Research Organization, Tsukuba, Japan
- ⁶⁶ Graduate School of Science, Kobe University, Kobe, Japan
- ⁶⁷ Faculty of Science, Kyoto University, Kyoto, Japan
- ⁶⁸ Kyoto University of Education, Kyoto, Japan
- ⁶⁹ Department of Physics, Kyushu University, Fukuoka, Japan
- ⁷⁰ Instituto de Física La Plata, Universidad Nacional de La Plata and CONICET, La Plata, Argentina
- ⁷¹ Physics Department, Lancaster University, Lancaster, United Kingdom
- ⁷² ^(a) INFN Sezione di Lecce; ^(b) Dipartimento di Matematica e Fisica, Università del Salento, Lecce, Italy
- ⁷³ Oliver Lodge Laboratory, University of Liverpool, Liverpool, United Kingdom
- ⁷⁴ Department of Physics, Jožef Stefan Institute and University of Ljubljana, Ljubljana, Slovenia
- ⁷⁵ School of Physics and Astronomy, Queen Mary University of London, London, United Kingdom
- ⁷⁶ Department of Physics, Royal Holloway University of London, Surrey, United Kingdom
- ⁷⁷ Department of Physics and Astronomy, University College London, London, United Kingdom
- ⁷⁸ Laboratoire de Physique Nucléaire et de Hautes Energies, UPMC and Université Paris-Diderot and CNRS/IN2P3, Paris, France
- ⁷⁹ Fysiska institutionen, Lunds universitet, Lund, Sweden
- ⁸⁰ Departamento de Física Teórica C-15, Universidad Autónoma de Madrid, Madrid, Spain
- ⁸¹ Institut für Physik, Universität Mainz, Mainz, Germany
- ⁸² School of Physics and Astronomy, University of Manchester, Manchester, United Kingdom
- ⁸³ CPPM, Aix-Marseille Université and CNRS/IN2P3, Marseille, France
- ⁸⁴ Department of Physics, University of Massachusetts, Amherst MA, United States of America
- ⁸⁵ Department of Physics, McGill University, Montreal QC, Canada
- ⁸⁶ School of Physics, University of Melbourne, Victoria, Australia
- ⁸⁷ Department of Physics, The University of Michigan, Ann Arbor MI, United States of America
- ⁸⁸ Department of Physics and Astronomy, Michigan State University, East Lansing MI, United States of America
- ⁸⁹ ^(a) INFN Sezione di Milano; ^(b) Dipartimento di Fisica, Università di Milano, Milano, Italy
- ⁹⁰ B.I. Stepanov Institute of Physics, National Academy of Sciences of Belarus, Minsk, Republic of Belarus
- ⁹¹ National Scientific and Educational Centre for Particle and High Energy Physics, Minsk, Republic of Belarus
- ⁹² Department of Physics, Massachusetts Institute of Technology, Cambridge MA, United States of America
- ⁹³ Group of Particle Physics, University of Montreal, Montreal QC, Canada
- ⁹⁴ P.N. Lebedev Institute of Physics, Academy of Sciences, Moscow, Russia
- ⁹⁵ Institute for Theoretical and Experimental Physics (ITEP), Moscow, Russia
- ⁹⁶ Moscow Engineering and Physics Institute (MEPhI), Moscow, Russia
- ⁹⁷ D.V.Skobel'syn Institute of Nuclear Physics, M.V.Lomonosov Moscow State University, Moscow, Russia
- ⁹⁸ Fakultät für Physik, Ludwig-Maximilians-Universität München, München, Germany
- ⁹⁹ Max-Planck-Institut für Physik (Werner-Heisenberg-Institut), München, Germany
- ¹⁰⁰ Nagasaki Institute of Applied Science, Nagasaki, Japan
- ¹⁰¹ Graduate School of Science and Kobayashi-Maskawa Institute, Nagoya University, Nagoya, Japan
- ¹⁰² ^(a) INFN Sezione di Napoli; ^(b) Dipartimento di Scienze Fisiche, Università di Napoli, Napoli, Italy
- ¹⁰³ Department of Physics and Astronomy, University of New Mexico, Albuquerque NM, United States of America
- ¹⁰⁴ Institute for Mathematics, Astrophysics and Particle Physics, Radboud University Nijmegen/Nikhef, Nijmegen, Netherlands
- ¹⁰⁵ Nikhef National Institute for Subatomic Physics and University of Amsterdam, Amsterdam, Netherlands
- ¹⁰⁶ Department of Physics, Northern Illinois University, DeKalb IL, United States of America
- ¹⁰⁷ Budker Institute of Nuclear Physics, SB RAS, Novosibirsk, Russia
- ¹⁰⁸ Department of Physics, New York University, New York NY, United States of America
- ¹⁰⁹ Ohio State University, Columbus OH, United States of America
- ¹¹⁰ Faculty of Science, Okayama University, Okayama, Japan
- ¹¹¹ Homer L. Dodge Department of Physics and Astronomy, University of Oklahoma, Norman OK, United States of America
- ¹¹² Department of Physics, Oklahoma State University, Stillwater OK, United States of America
- ¹¹³ Palacký University, RCPTM, Olomouc, Czech Republic

- 114 Center for High Energy Physics, University of Oregon, Eugene OR, United States of America
 115 LAL, Université Paris-Sud and CNRS/IN2P3, Orsay, France
 116 Graduate School of Science, Osaka University, Osaka, Japan
 117 Department of Physics, University of Oslo, Oslo, Norway
 118 Department of Physics, Oxford University, Oxford, United Kingdom
 119 (a) INFN Sezione di Pavia; (b) Dipartimento di Fisica, Università di Pavia, Pavia, Italy
 120 Department of Physics, University of Pennsylvania, Philadelphia PA, United States of America
 121 Petersburg Nuclear Physics Institute, Gatchina, Russia
 122 (a) INFN Sezione di Pisa; (b) Dipartimento di Fisica E. Fermi, Università di Pisa, Pisa, Italy
 123 Department of Physics and Astronomy, University of Pittsburgh, Pittsburgh PA, United States of America
 124 (a) Laboratório de Instrumentação e Física Experimental de Partículas - LIP, Lisboa, Portugal; (b) Departamento de Física Teórica y del Cosmos and CAFPE, Universidad de Granada, Granada, Spain
 125 Institute of Physics, Academy of Sciences of the Czech Republic, Praha, Czech Republic
 126 Czech Technical University in Prague, Praha, Czech Republic
 127 Faculty of Mathematics and Physics, Charles University in Prague, Praha, Czech Republic
 128 State Research Center Institute for High Energy Physics, Protvino, Russia
 129 Particle Physics Department, Rutherford Appleton Laboratory, Didcot, United Kingdom
 130 Physics Department, University of Regina, Regina SK, Canada
 131 Ritsumeikan University, Kusatsu, Shiga, Japan
 132 (a) INFN Sezione di Roma I; (b) Dipartimento di Fisica, Università La Sapienza, Roma, Italy
 133 (a) INFN Sezione di Roma Tor Vergata; (b) Dipartimento di Fisica, Università di Roma Tor Vergata, Roma, Italy
 134 (a) INFN Sezione di Roma Tre; (b) Dipartimento di Matematica e Fisica, Università Roma Tre, Roma, Italy
 135 (a) Faculté des Sciences Ain Chock, Réseau Universitaire de Physique des Hautes Energies - Université Hassan II, Casablanca; (b) Centre National de l'Énergie des Sciences Techniques Nucleaires, Rabat; (c) Faculté des Sciences Semlalia, Université Cadi Ayyad, LPHEA-Marrakech; (d) Faculté des Sciences, Université Mohamed Premier and LPTPM, Oujda; (e) Faculté des sciences, Université Mohammed V-Agdal, Rabat, Morocco
 136 DSM/IRFU (Institut de Recherches sur les Lois Fondamentales de l'Univers), CEA Saclay (Commissariat à l'Énergie Atomique et aux Énergies Alternatives), Gif-sur-Yvette, France
 137 Santa Cruz Institute for Particle Physics, University of California Santa Cruz, Santa Cruz CA, United States of America
 138 Department of Physics, University of Washington, Seattle WA, United States of America
 139 Department of Physics and Astronomy, University of Sheffield, Sheffield, United Kingdom
 140 Department of Physics, Shinshu University, Nagano, Japan
 141 Fachbereich Physik, Universität Siegen, Siegen, Germany
 142 Department of Physics, Simon Fraser University, Burnaby BC, Canada
 143 SLAC National Accelerator Laboratory, Stanford CA, United States of America
 144 (a) Faculty of Mathematics, Physics & Informatics, Comenius University, Bratislava; (b) Department of Subnuclear Physics, Institute of Experimental Physics of the Slovak Academy of Sciences, Kosice, Slovak Republic
 145 (a) Department of Physics, University of Johannesburg, Johannesburg; (b) School of Physics, University of the Witwatersrand, Johannesburg, South Africa
 146 (a) Department of Physics, Stockholm University; (b) The Oskar Klein Centre, Stockholm, Sweden
 147 Physics Department, Royal Institute of Technology, Stockholm, Sweden
 148 Departments of Physics & Astronomy and Chemistry, Stony Brook University, Stony Brook NY, United States of America
 149 Department of Physics and Astronomy, University of Sussex, Brighton, United Kingdom
 150 School of Physics, University of Sydney, Sydney, Australia
 151 Institute of Physics, Academia Sinica, Taipei, Taiwan
 152 Department of Physics, Technion: Israel Institute of Technology, Haifa, Israel
 153 Raymond and Beverly Sackler School of Physics and Astronomy, Tel Aviv University, Tel Aviv, Israel
 154 Department of Physics, Aristotle University of Thessaloniki, Thessaloniki, Greece
 155 International Center for Elementary Particle Physics and Department of Physics, The University of Tokyo, Tokyo, Japan
 156 Graduate School of Science and Technology, Tokyo Metropolitan University, Tokyo, Japan
 157 Department of Physics, Tokyo Institute of Technology, Tokyo, Japan
 158 Department of Physics, University of Toronto, Toronto ON, Canada

- ¹⁵⁹ (a) TRIUMF, Vancouver BC; (b) Department of Physics and Astronomy, York University, Toronto ON, Canada
- ¹⁶⁰ Faculty of Pure and Applied Sciences, University of Tsukuba, Tsukuba, Japan
- ¹⁶¹ Department of Physics and Astronomy, Tufts University, Medford MA, United States of America
- ¹⁶² Centro de Investigaciones, Universidad Antonio Narino, Bogota, Colombia
- ¹⁶³ Department of Physics and Astronomy, University of California Irvine, Irvine CA, United States of America
- ¹⁶⁴ (a) INFN Gruppo Collegato di Udine; (b) ICTP, Trieste; (c) Dipartimento di Chimica, Fisica e Ambiente, Università di Udine, Udine, Italy
- ¹⁶⁵ Department of Physics, University of Illinois, Urbana IL, United States of America
- ¹⁶⁶ Department of Physics and Astronomy, University of Uppsala, Uppsala, Sweden
- ¹⁶⁷ Instituto de Física Corpuscular (IFIC) and Departamento de Física Atómica, Molecular y Nuclear and Departamento de Ingeniería Electrónica and Instituto de Microelectrónica de Barcelona (IMB-CNM), University of Valencia and CSIC, Valencia, Spain
- ¹⁶⁸ Department of Physics, University of British Columbia, Vancouver BC, Canada
- ¹⁶⁹ Department of Physics and Astronomy, University of Victoria, Victoria BC, Canada
- ¹⁷⁰ Department of Physics, University of Warwick, Coventry, United Kingdom
- ¹⁷¹ Waseda University, Tokyo, Japan
- ¹⁷² Department of Particle Physics, The Weizmann Institute of Science, Rehovot, Israel
- ¹⁷³ Department of Physics, University of Wisconsin, Madison WI, United States of America
- ¹⁷⁴ Fakultät für Physik und Astronomie, Julius-Maximilians-Universität, Würzburg, Germany
- ¹⁷⁵ Fachbereich C Physik, Bergische Universität Wuppertal, Wuppertal, Germany
- ¹⁷⁶ Department of Physics, Yale University, New Haven CT, United States of America
- ¹⁷⁷ Yerevan Physics Institute, Yerevan, Armenia
- ¹⁷⁸ Centre de Calcul de l'Institut National de Physique Nucléaire et de Physique des Particules (IN2P3), Villeurbanne, France
- ^a Also at Department of Physics, King's College London, London, United Kingdom
- ^b Also at Laboratorio de Instrumentacao e Fisica Experimental de Particulas - LIP, Lisboa, Portugal
- ^c Also at Faculdade de Ciencias and CFNUL, Universidade de Lisboa, Lisboa, Portugal
- ^d Also at Particle Physics Department, Rutherford Appleton Laboratory, Didcot, United Kingdom
- ^e Also at TRIUMF, Vancouver BC, Canada
- ^f Also at Department of Physics, California State University, Fresno CA, United States of America
- ^g Also at Novosibirsk State University, Novosibirsk, Russia
- ^h Also at Department of Physics, University of Coimbra, Coimbra, Portugal
- ⁱ Also at Università di Napoli Parthenope, Napoli, Italy
- ^j Also at Institute of Particle Physics (IPP), Canada
- ^k Also at Department of Physics, Middle East Technical University, Ankara, Turkey
- ^l Also at Louisiana Tech University, Ruston LA, United States of America
- ^m Also at Dep Fisica and CEFITEC of Faculdade de Ciencias e Tecnologia, Universidade Nova de Lisboa, Caparica, Portugal
- ⁿ Also at Department of Physics and Astronomy, Michigan State University, East Lansing MI, United States of America
- ^o Also at Department of Physics, University of Cape Town, Cape Town, South Africa
- ^p Also at Institute of Physics, Azerbaijan Academy of Sciences, Baku, Azerbaijan
- ^q Also at Institut für Experimentalphysik, Universität Hamburg, Hamburg, Germany
- ^r Also at Manhattan College, New York NY, United States of America
- ^s Also at CPPM, Aix-Marseille Université and CNRS/IN2P3, Marseille, France
- ^t Also at School of Physics and Engineering, Sun Yat-sen University, Guanzhou, China
- ^u Also at Academia Sinica Grid Computing, Institute of Physics, Academia Sinica, Taipei, Taiwan
- ^v Also at Laboratoire de Physique Nucléaire et de Hautes Energies, UPMC and Université Paris-Diderot and CNRS/IN2P3, Paris, France
- ^w Also at School of Physical Sciences, National Institute of Science Education and Research, Bhubaneswar, India
- ^x Also at Dipartimento di Fisica, Università La Sapienza, Roma, Italy
- ^y Also at DSM/IRFU (Institut de Recherches sur les Lois Fondamentales de l'Univers), CEA Saclay (Commissariat à l'Énergie Atomique et aux Énergies Alternatives), Gif-sur-Yvette, France
- ^z Also at Section de Physique, Université de Genève, Geneva, Switzerland
- ^{aa} Also at Departamento de Fisica, Universidade de Minho, Braga, Portugal
- ^{ab} Also at Department of Physics, The University of Texas at Austin, Austin TX, United States of America
- ^{ac} Also at Department of Physics and Astronomy, University of South Carolina, Columbia SC, United States of

America

^{ad} Also at Institute for Particle and Nuclear Physics, Wigner Research Centre for Physics, Budapest, Hungary

^{ae} Also at DESY, Hamburg and Zeuthen, Germany

^{af} Also at International School for Advanced Studies (SISSA), Trieste, Italy

^{ag} Also at LAL, Université Paris-Sud and CNRS/IN2P3, Orsay, France

^{ah} Also at Faculty of Physics, M.V.Lomonosov Moscow State University, Moscow, Russia

^{ai} Also at Nevis Laboratory, Columbia University, Irvington NY, United States of America

^{aj} Also at Department of Physics, Oxford University, Oxford, United Kingdom

^{ak} Also at Discipline of Physics, University of KwaZulu-Natal, Durban, South Africa

* Deceased